

From: Yeilding, Cindy
Sent: Thu May 27 01:14:44 2010
To: Rainey, David I; Thorseth, Jay C; Walz, Gregory S; Chester, Doug K; Grant, James R; Zwart, Peter A
Cc: Vinson, Graham (Pinky); Walton, Gene; Ritchie, Bryan; Sprague, Jonathan D; O'Bryan, Patrick L;
Sims, David C; Frazelle, Andrew E; MC252_Email_Retention@bp.com.; Baker, Kate H (UNKNOWN
BUSINESS PARTNER); Peijs, Jasper
Subject: INFO: Objectives and Delivery, MC 252 (Macondo), May 25th-26th, 2010
Importance: Normal
Attachments: MC252 Subsurface Technical Memo v1.doc; Macondo SIWHP Build-up Rate Final Report
Rev D.doc

Dear all,
MC 252 Relief wells:

- Integrated Asset View session delivered by P. Johnston; enables real-time monitoring of both wells.

\\Cis3.hou.pce.bp.com\gomdx\scat04\gomdxt\johnston\Macondo
RX-C (DDIII, MC 252-3): Bryan Ritchie

- Tagged cement at 9820' md, hole depth 10,100 md
- Next step: test BOP

RxD Well, DDII, MC 252-2: Gene Walton

- Cement 22" casing, TD 8575'
- Next step: T&A

Subsurface Analysis: Bryan Ritchie

- Subsurface report/post-well, draft 1: data compilation
<<...>>

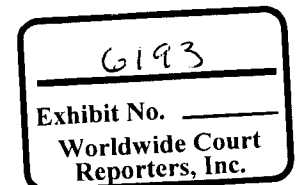
Macondo Fluids: (K. McAughan, D. Kercho)

- Provided gas and oil relief flow rates to maintain a constant wellhead pressure of 9000psi.
- Provided Jasper Peijs with MDT raw data, sand description with reservoir, reservoir log (picture), up-to-date fluid data for UT/NOAA analysis.

Shut In Well Head Pressure (D. Kercho, K. McAughan, R. Merrill, M. Mason and EPTG
team members)

- Provided Phil Pattillo with reservoir pressure at abandonment.
- Chris Cecil revised previous SIWHP document to reflect work done by US National Laboratories and incorporated some minor edits

<<...>>



CONFIDENTIAL

BP-HZN-2179MDL00646495

BPD136-005655

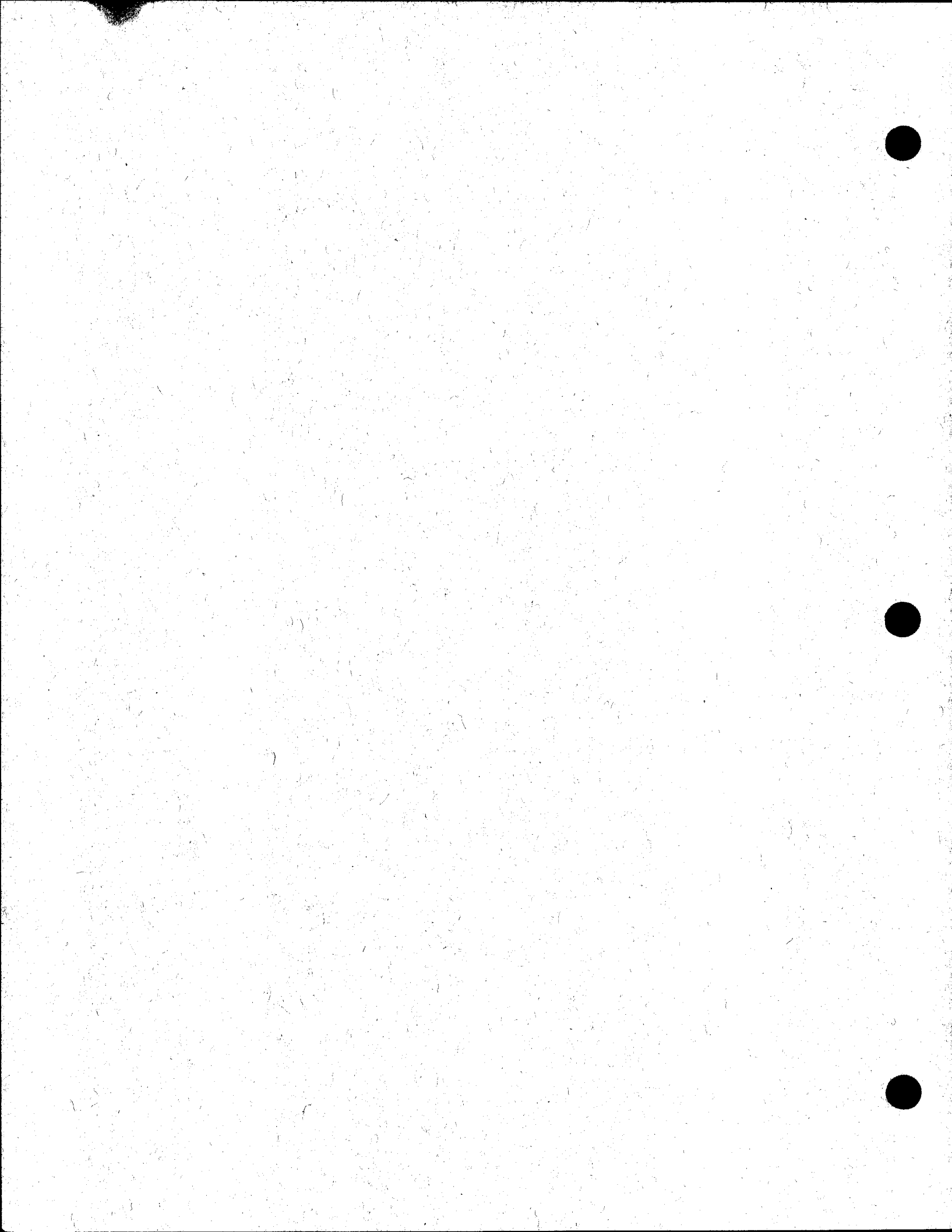
ROV Seabed monitoring: A. Hill

- Seabed monitoring with ROVs considered by IMT but seen as operationally too difficult (P. Tooms/K. Baker)

Leadership Support:

- Provided TAM production rate/profiles and technical support for D. Rainey/J. Morgheim
- Request for Geochemical support, full-time, from P. Carragher to J. Barton







Technical Memorandum

TITLE: Post-Well Subsurface Description of Macondo well (MC 252)

TO: Kate Baker, Cindy Yeilding, Jay Thorseth, Peter Carragher

WRITTEN BY: Marty Albertin, Chuck Bondurant, Kelly McAughan, Binh van Nguyen
Bryan Ritchie, Craig Scherschel, Galina Skripnikova

DATE: 25th May 2010

Introduction

This technical memorandum outlines the post-well subsurface description of the Macondo well in Mississippi Canyon Block 252 (OCS-G-32306) in the north-central Gulf of Mexico.

| | |
|---|---|
| Prospect Name | Macondo |
| Surface Location Block No. | Mississippi Canyon 252 |
| BP well name | MC 252_1 |
| OCS-G Well number | OCS - G32306_01 |
| Spud date on Marianas | 6 th October 2009 |
| Released Marianas due to Hurricane Ida | 27 th November 2009 |
| Re-entered well on Deepwater Horizon | 10 th February 2010 |
| Category (Exp/Appr) | Exploration |
| Total Depth (MD/TVD/TVSS) | 18,360' md / 18,349' tvd / -18,274' tvdss |
| EP Approved by MMS | 04/06/2009 |
| Water Depth | 4,992 feet |
| Rotary Table Elevation | 75 feet RKB |
| Top Reservoir Depth | 18,065' md / 18,054' tvd / -17,965' tvdss |
| Net Reservoir Thickness | 90 ft |
| Reservoir Temperature | 236° F |
| Reservoir Pressure | 11,850 psi |
| GOR | 3,000 scf/bbl |
| API | 35 |

Macondo spud
October 6, 2009

Marianas pulled off location

November 27, 2009

After running the 18" casing and cementing the same, the Marianas BOP failed a scheduled test. At the time of the failed test, the 18" casing had been run and cemented. No open hole was exposed. A cement plug was set in the 28" casing, and the riser/BOP stack was pulled. While the BOP stack was being repaired on deck, the late season hurricane Ida formed in the gulf. The well location was in the projected path of the hurricane. The Marianas was evacuated. Upon returning to the rig after the storm, inspections had revealed extensive damage to wire/cables along the underside of the rig. These wires/cables were damaged as the result of waves/swells impacting the underside of the hull. This caused the sheathing of many of the wires/cables to be worn to the point that bare wires were exposed. After assessing the situation it was deemed that the damage was too extensive to perform repairs on location. The rig was de-moored and towed to a shipyard in Mississippi to perform the requisite repairs. While being repaired in the shipyard, the rig contract expired. After finishing repairs, the rig was released.

Well status at time the Marianas was pulled off location

The 18" casing was run and cemented. A 200' cement plug was set near the 28" casing shoe. It was decided that the Deepwater Horizon would finish drilling the Macondo well after finishing appraisal drilling operations at the Kodiak discovery.

On location with the Deepwater Horizon

January 31, 2010

After performing scheduled drawworks and BOP maintenance, running the riser, and testing the BOP on the wellhead, the Macondo well was re-entered on February 10, 2010. Upon re-entry, the cement plug set by the Marianas was drilled-out. After squeezing the 18" casing shoe, the Deepwater Horizon began making new hole on February 15, 2010.

Date encountered and depth of main target

The primary M56 target was encountered on April 4, 2010 while drilling at a depth of 18,065' (MD)/18,054' (TVD).

Date and depth of final TD

The Macondo well reached a final TD of 18,360' (MD)/18,349' (TVD) on April 9, 2010.

Post-TD operations

After reaching TD, a full suite of wireline evaluation was performed. Following wireline operations, production casing was run and cemented. At the time of the incident, the riser was being displaced to seawater in preparation to unlatch from the wellhead and pull the riser/BOP stack.

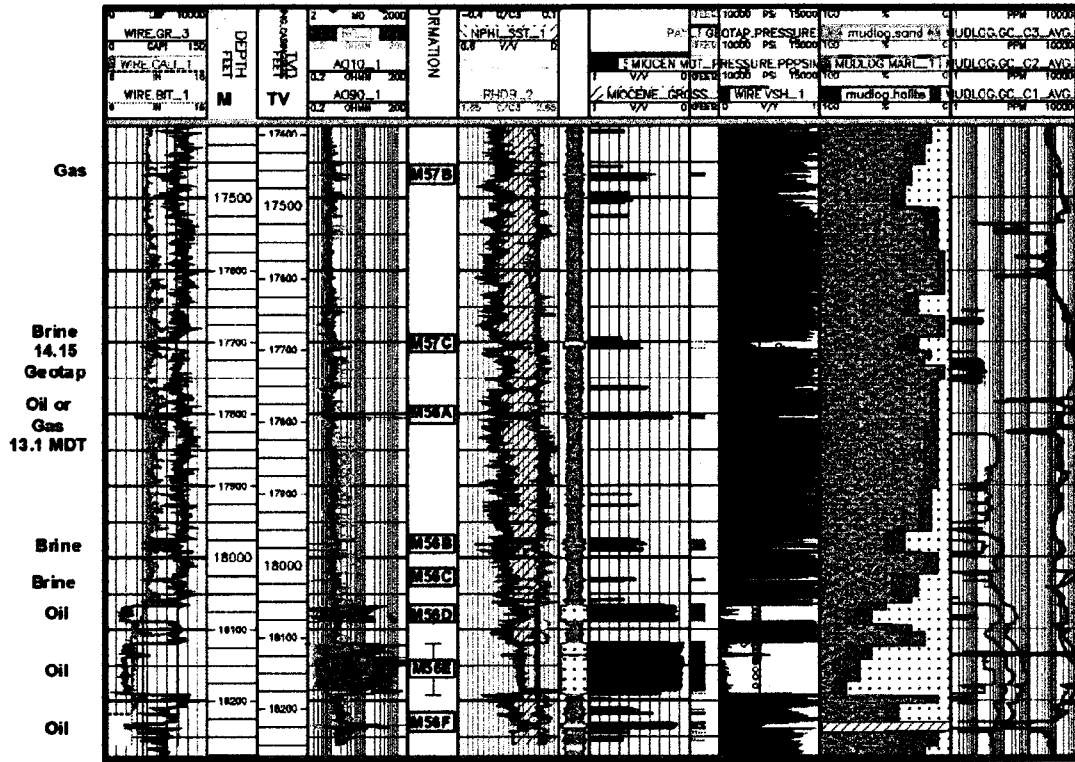


Figure 2: Sand identification chart for sands below the 9-7/8" liner that were cut by the MC0252_1BP1 well.

M56 Depth and Brine/Oil Distribution Maps

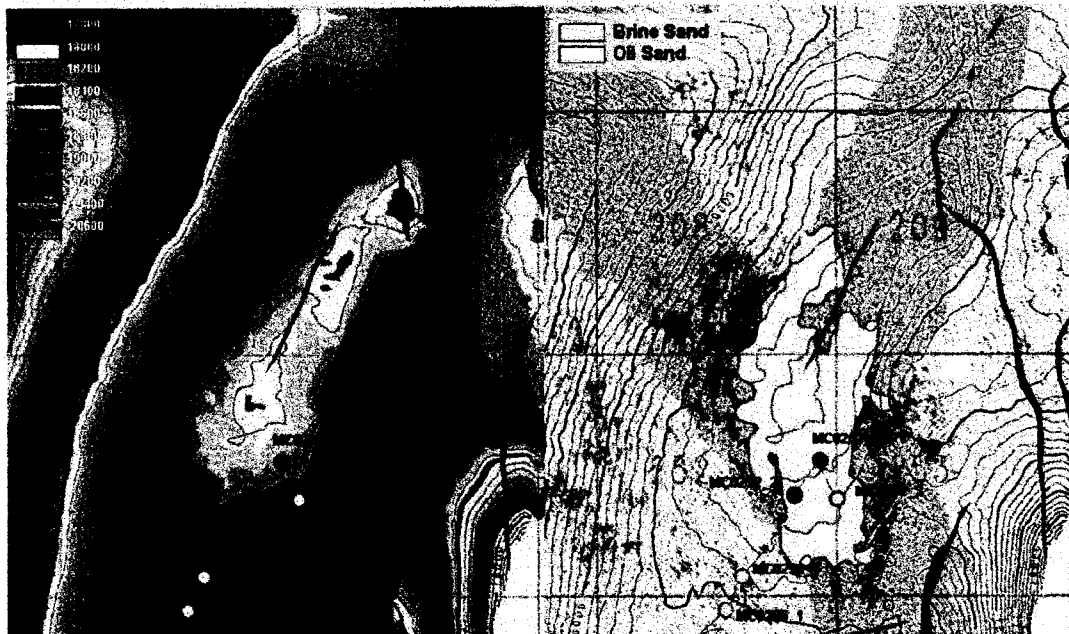


Figure 3: M56 Depth Structure Map and Amplitude Map.

Rigel field

Approximately 1 to 3 miles to the south-west of the Macondo well is a series of five channel-levee complexes. These channel sands range in depths from 9100ft TVDSS to 14,000ft TVDSS. The Rigel field produces biogenic gas from one of the channel systems (Figure 5).

The Rigel field is a shallow (~11,000') biogenic gas field in south-central Mississippi Canyon block #252. It is approximately M72 in age. The original Rigel exploration well was drilled by Texaco in 1999 to a TD of 13,600' (MD)/12,832' (TVD). Subsequently, a production well was drilled in 2003 by Dominion E&P. This well reached a TD of 16,200' (MD)/14,162' (TVD). This well is drilled from block 252 directionally toward the southwest. The bottom-hole location is in Mississippi Canyon block #296. This well is completed in a single zone around 11,000' (TVD). As of the middle of last year, the well has produced 72.5bcf dry gas. It is exported via the Rigel pipeline. The well is currently operated by ENI.

Seismic evidence shows that the lateral extent of the closest of these channel-levee systems (M110) does not reach the Macondo well (Figure 6).

M57 Depth and Brine/Oil Distribution Maps



Figure 4: M57 Depth Structure Map and Amplitude Map.

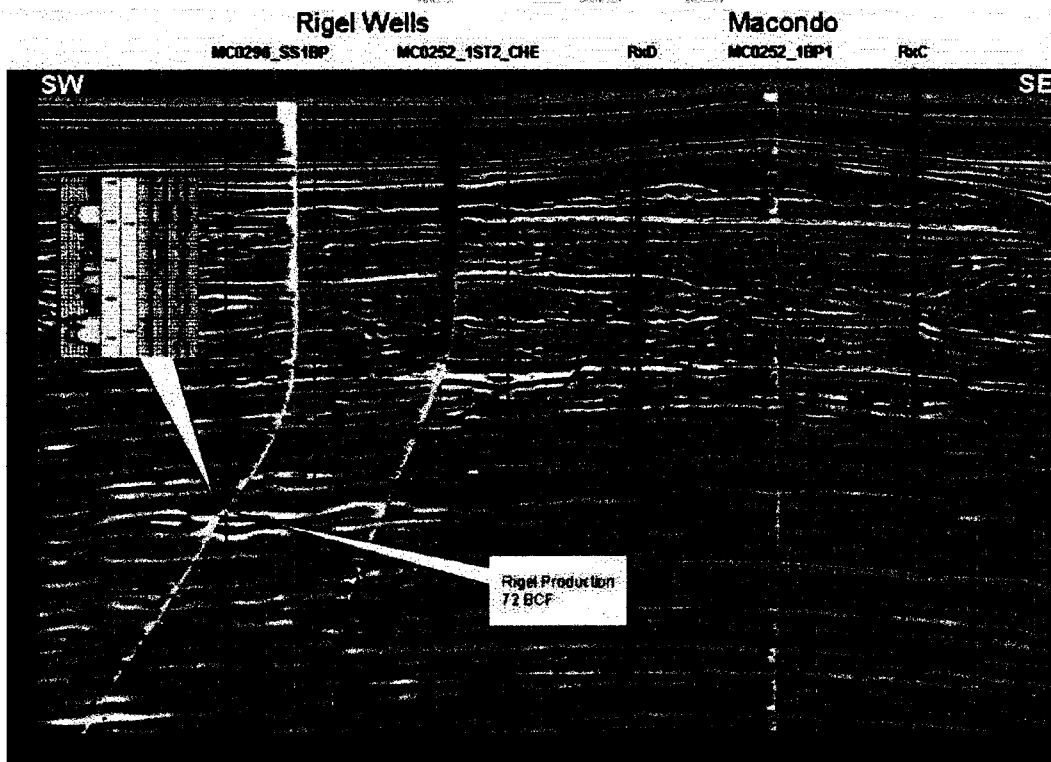


Figure 5: Seismic section showing Rigel wells and Macondo.

Version 1

BP Confidential

6

M110 Depth and Brine/Oil Distribution Maps

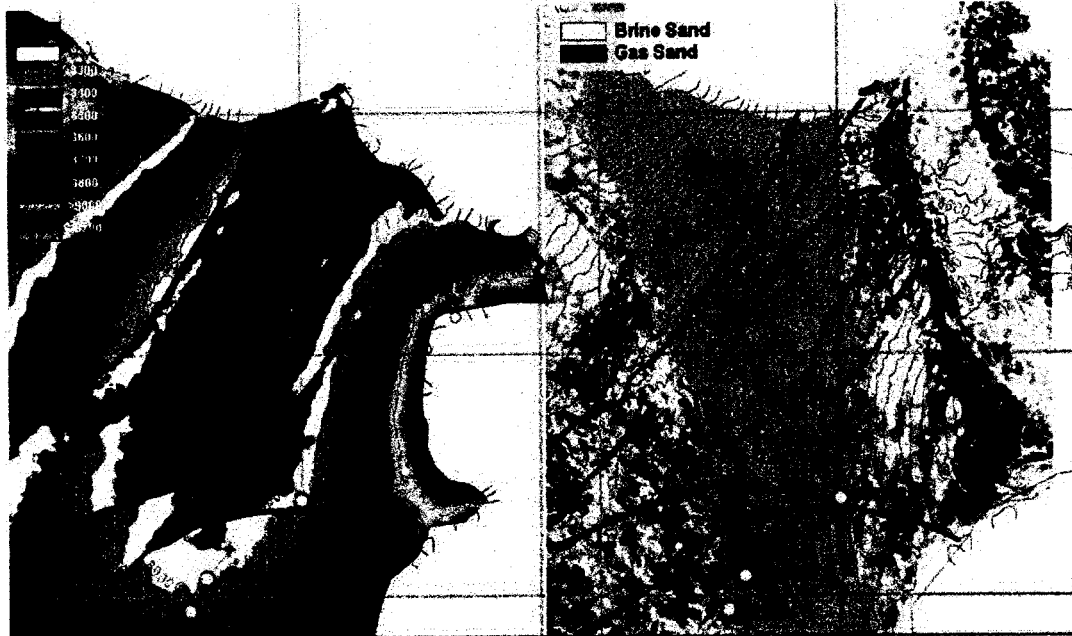


Figure 6: M110 Depth Structure Map and Amplitude Map

Shallow Hazards

BP completed an archaeological and seafloor geohazards survey across Mississippi Canyon Block 252 and vicinity in January 2009 to meet MMS requirements for archaeologically significant blocks. No significant man-made or natural hazards were identified near the proposed MC 252-1 well or within the proposed anchor radius for the Marianas drilling rig.

The shallow hazards discussion is limited to the top-hole or riserless section (i.e. between seafloor and the base of the 22-inch casing section). Figure 7 shows the top-hole formation forecast (THFF) for shallow geohazards that was derived from 3D seismic data. Figure 8 shows the shallow hazards top-hole observations log that was generated after drilling the top-hole section. The post-well comparison between actual drilling conditions and pre-drill prediction is provided below.

Shallow Gas

The zone from the seafloor to 8,001 ft MD (base of 22-inch casing section) was predicted to have a Negligible potential of shallow gas. No shallow gas was observed while drilling the riserless section.

Shallow Water Flow

A Low risk for SWF was assessed for two intervals (6,570 ft to 6,701 ft MD and 7,025 ft to 7,614 ft MD). There was one unit predicted with a Moderate risk of encountering SWF in the pre-drill THFF between 6,913 ft and 7,025 ft MD. Although sand-prone intervals are noted from the gamma log between 6,660 ft to 6,900 ft and 6,950 ft to 7,080 ft, no SWF was noted while drilling the riserless section.

A slight flow was noted across the top of the wellhead about 50 hrs after reaching the total depth (TD) of the 22-inch casing section while tripping in hole with the 22-inch casing. It is assumed that the slight flow may have come from possible sands noted above. The flow was stopped by circulating mud.

Hydrates

The potential for gas hydrates was predicted as Negligible-Low for the entire riserless section. There was no visual evidence or log data that indicated possible gas hydrates while drilling the riserless section.

Gumbo

The potential for gumbo shale, a plastic clay return response to water based mud, was not addressed in the pre-drill THFF. This was not a concern because the plan was to drill the hole section with seawater. Gumbo was observed towards the end of drilling the 22-inch casing hole section. The gumbo coincided with circulating pad mud in place in preparation of running casing.

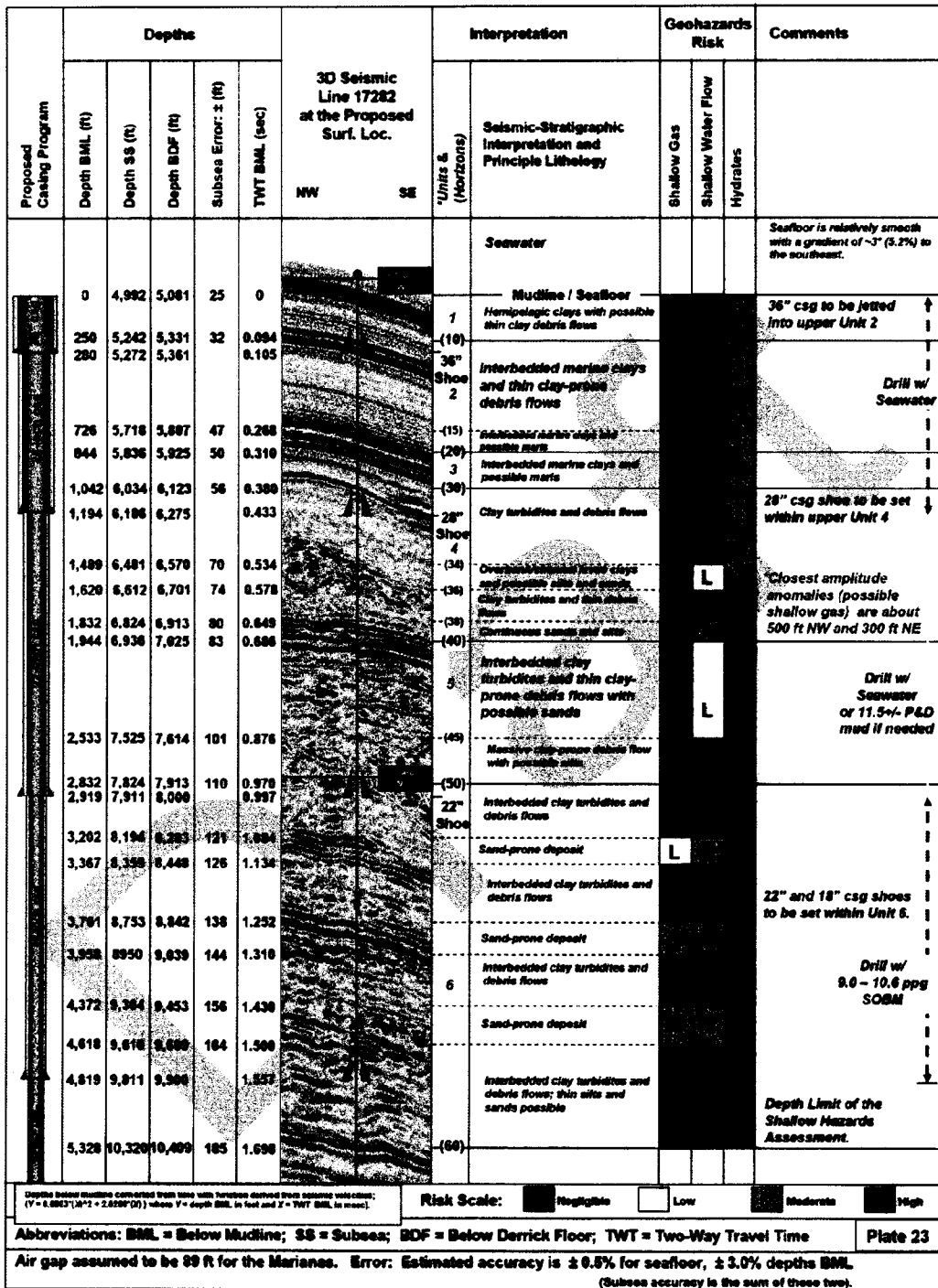


Figure 7: Original Top-Hole Formation Forecast at the Proposed MC-252 #1 Location (produced by Craig A. Scherschel, 08 June 2009).



**MC 252 #1 (Macondo) LWD Log
with Shallow Hazards Observations**

WELL LOCATION: Proposed MC 252 Location
AREA: Mississippi Canyon 252
WELL API: 60817 41169 00
DATE: 6-10 Oct 2009

EASTING: 1,202,796.33 FT
NORTHING: 10,431,619.79 FT
DATUM: NAD 1927; Spheroid: Clarke 1866
PROJECTION: UTM Zone 18N (ft)

Pre - Drill Assessment
Predicted Seabed Depth
Water Depth = 4,992' SS

Post - Drill Observations
Measured Depth (Air Gap = 89 ft)
Water Depth = 4,992' SS

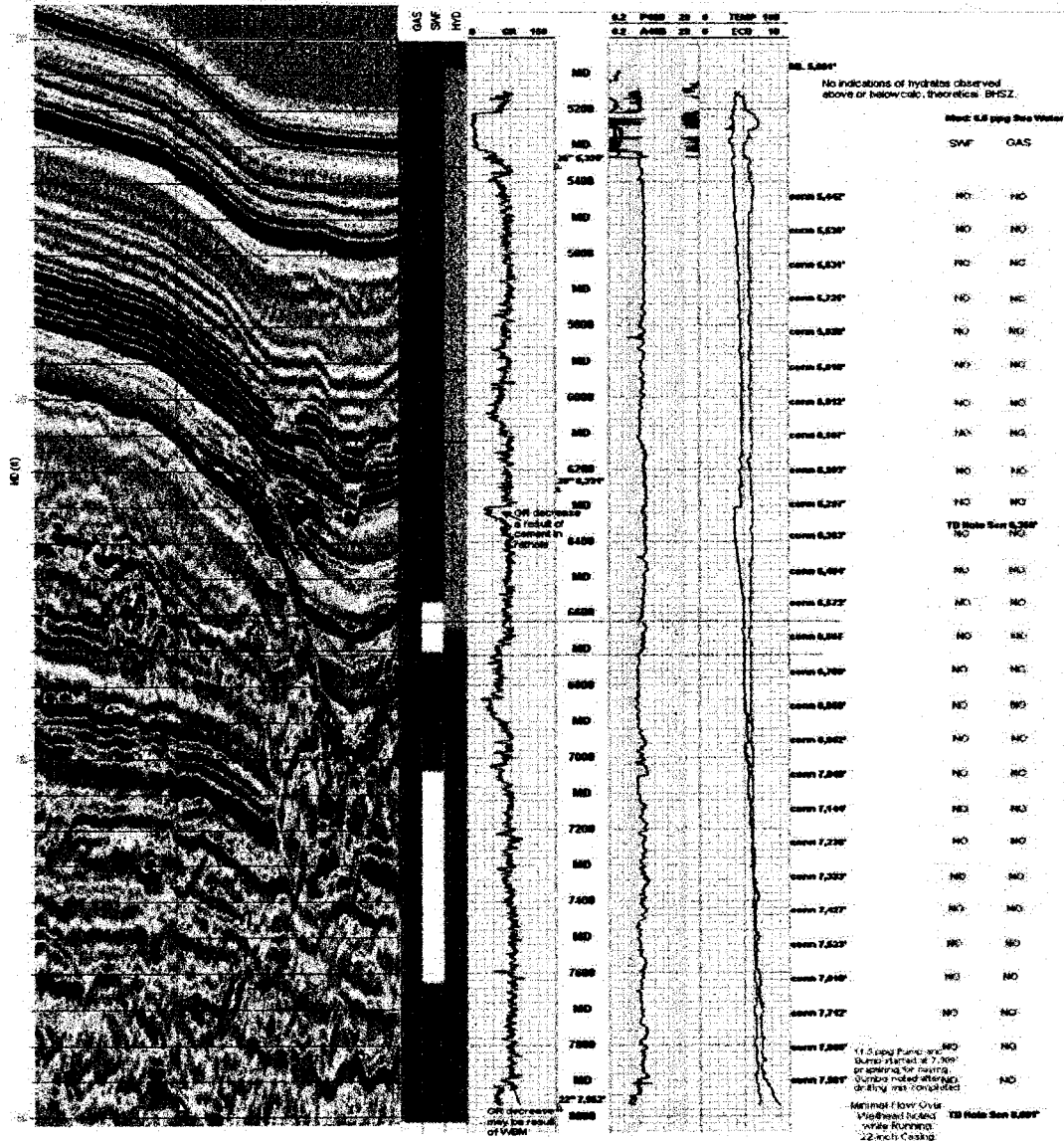


Figure 8: Shallow Hazards Top-hole Observations Log for the MC-252 #1 Location between Seafloor and the Base of the 22-inch Casing Hole Section (produced by Kate Paine, October 2009).

Pore Pressure and Fracture Gradient

The current Macondo pressure interpretation incorporates revisions to the pre-drill forecast based on: synthesis of LWD and wireline pressure indicators (pressure transforms based on resistivity, sonic and checkshot, and density); drilling parameters and data (RxC, background and connection gases), direct drilling indicators (kicks, losses), and GeoTap and MDT pressure measurements (Figure 9). Pore pressure is higher than the predrill most likely curve, from 9000' to 17750' TVDKB. The pre-drill pressure prediction was too low in this interval due to slower than predicted interval velocities, and the apparent need for higher pressure transform model more similar to that used in the analysis of the high pressure, narrow margin offset well "Yumuri", MC382-1. Reservoir pressures are much lower than predicted. Pre-drill centroid modeling of channel sands draped over the large 4-way Macondo structure placed reservoir pressures 0.1-0.3 ppg higher than shale pressure. Actual reservoir pressures imply regional hydraulic connectivity to deeper water, lower overburden/pore pressure environments to the south (similar reservoir pressure to Isabella), or local connectivity updip beneath the salt bodies southwest and east of the prospect. Though wireline density is limited to the reservoir section, calibrated acoustic to density transforms of the Macondo sonic and checkshot imply that overburden is lower than predicted. Lower densities used in the calibrated postwell overburden are consistent with the higher than predicted pore pressure observed at the prospect. The narrower than predicted PPFG window above the reservoir level led to shallower than planned shoes, and use of contingency liners.

Macondo MC_252-1-A Pressure Forecast: REV3 , 5/17/10

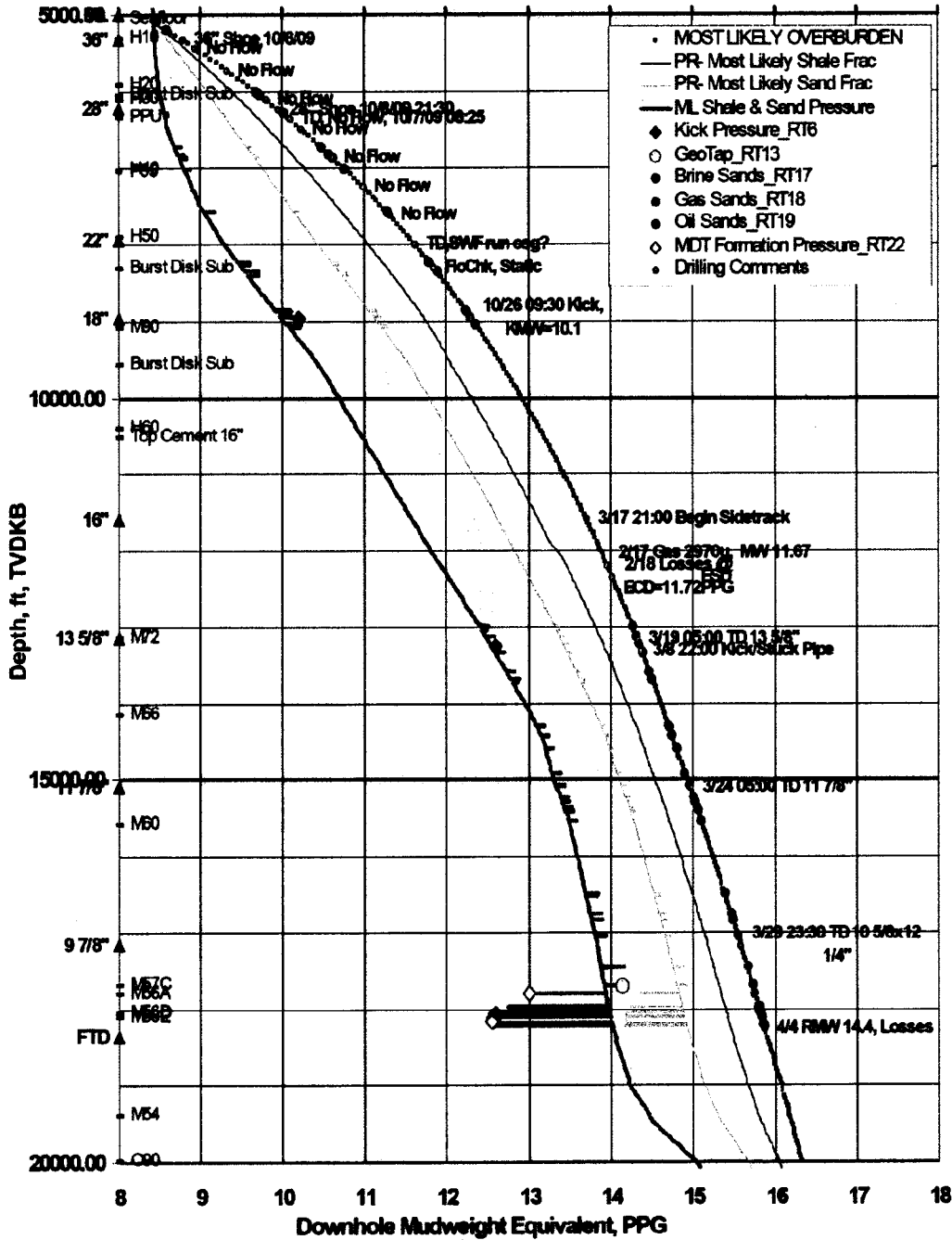


Figure 9: Post-well PPFG interpretation.

Petrophysics

Summary

From shows, log response and fluid samples it is interpreted that >90 feet of hydrocarbons were discovered in the M57 and M56 sands, the majority occurring in the M56D (22') and M56E (64.5') sands. Porosity averages 22%, Sw averages 10 - 17% and permeability averages in the range of 250 - 500 mD (arithmetic, log derived).

Fluid sample quality is high - volatile oil with GOR ~3000 and API=35, PVT analysis showed viscosity of 0.17 cp.

No hydrocarbon-water contacts were penetrated and no significant aquifer sandstone was observed.

Log derived porosity and permeability were calibrated to data from rotary side wall core sample analysis.

M56D is probably slightly different rock type and more heterogeneous than M56E, this is supported by core and log data.

The successful calibration of log data to core plug data in the M56E sand gives a reasonably high degree of certainty around the petrophysical parameters despite the relative lack of core data. A greater degree of uncertainty exists in the more heterogeneous M56D sand. Further uncertainty exists in the thin minor hydrocarbon bearing intervals in M56 and M57. They were not covered by core data and are difficult to resolve with standard logging tools as they are less than 2.5 feet in thickness. The lowest M56F sand was not fully covered by logs.

Electrical properties, capillary pressure data and thin section analysis will be incorporated into the interpretation when available.

Data base

All LWD, Wireline, Mud logging, Pressure and Core data was loaded into Geolog where formation evaluation was completed.

LWD

Halliburton was the Logging While Drilling (LWD) vendor. GR, Resistivity, Sonic and PWD tools were in the BHA while drilling plus Geotap formation pressure in target section.

In the wireline section, LWD was depth shifted to TCOMBO Gamma Ray. In cased hole section, where wireline Sonic in casing was run, LWD was shifted to it to match sonic response on LWD and wireline. From mudline to top of sonic in casing (~11,700' md) the depth shift was distributed.

Wireline

The following Schlumberger open hole wireline logs were run in 6 descents in open hole section from 17,150'-18,270' MD. They include the following tools:

R1D1: ZAIT-GPIT-LDS-CNL-GR-LEHQT
R1D2: CMR-ECS-HNGS-LEHQT
R1D3: Dual OBMI-GPIT-DSI-GR-LEHQT
R1D4: MDT-GR-LEHQT (pressure and samples)

Version 1

BP Confidential

13

R1D5: MSCT-GR-LEHQT (rotary side wall cores) was not fully successful; repeated as R1D7 after R1D6
R1D6: Quad VSI-GR-LEHQT

Basic observation on logs and borehole condition:

- The hole has a diameter of 8.5" from TD of 18270' to 18,090' md and 9.875" from 18,090' md to the 9.875" casing due to the use of a hole opener assembly.
- This hole section was drilled with barite as a mud weighting material (~20 % of high gravity weight solids). This causes the density correction curve (DRHO) to read negative and also significantly affects the quality of the PEF curve.
- Run R1D1 was run ~7 days after the formation was drilled and 20 hours after the last circulation stopped. During that time the open hole was exposed to different kinds LCM materials to treat losses, below the 9.875" shoe and close to TD. The caliper indicates some wash outs in shales but mainly gauge hole in sandstone.

Core

There were 44 rotary side wall core samples recovered from 3 MSCT runs. Sample preparation and analyses were done at Weatherford's Laboratories.

Only around 2/3rds of the samples were in a condition suitable for petrophysical analysis. After sufficient cleaning and drying, 6 samples were dedicated for mechanical properties and pore compressibility studies. 19 samples were selected for Routine Core Analysis (RCA). The analyses from 17 samples from M56D and M56E have been completed to date and are referenced in this document whilst 2 more sample are still being analysed. RCA was performed at 500 psi and at Net Confining Stress (NCS) of 2000 psi. NCS was calculated from post well sand fracture evaluation, over burden estimation and pore pressure.

If the assumption is made that one sample describes one inch of rock, the core plus represent approximately 2% of the M56D unit and 1.4% of the M56E in terms of amount of interval covered.

Currently Special Core analysis (Electrical Properties and Capillary pressure measurements) are been run on a set of samples

16 out of the 17 samples were described as fine to medium size grain sandstones, one as shale.

Laser Grain Size Analysis (LGSA) results on 17 samples (6 in M56D and 11 in M56E) are presented in Figures 10 and 11.

In Figure 10 Klinkenberg corrected permeability to air at NCS is plotted versus the percentage of different size particles in the sample. There is a clear relationship between sand content and permeability.

It could be argued that the M56D samples (green) have marginally more silt and less sand grain size particles than M56E samples (blue), though with the relatively small data set this may be a function of the sampling.

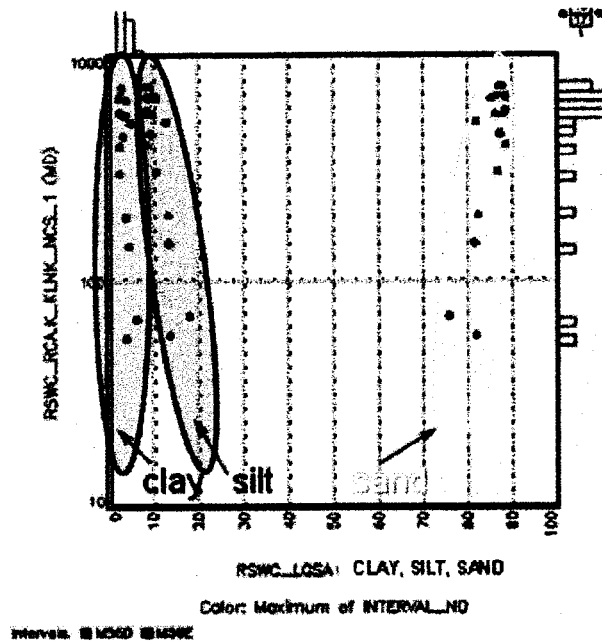


Figure 10: Laser Grain Size Analysis, Permeability vs. percentage of different (sand, silt, clay) size particles.

In Figure 11 Klinkenberg permeability to air at NGS is plotted versus percentage of different size sand particles. The data shows a clear relationship between grain size and permeability. In general M56D (green) has a subtly wider range of grain size suggesting slightly poor sorting, while the M56E (blue) is more homogeneous.

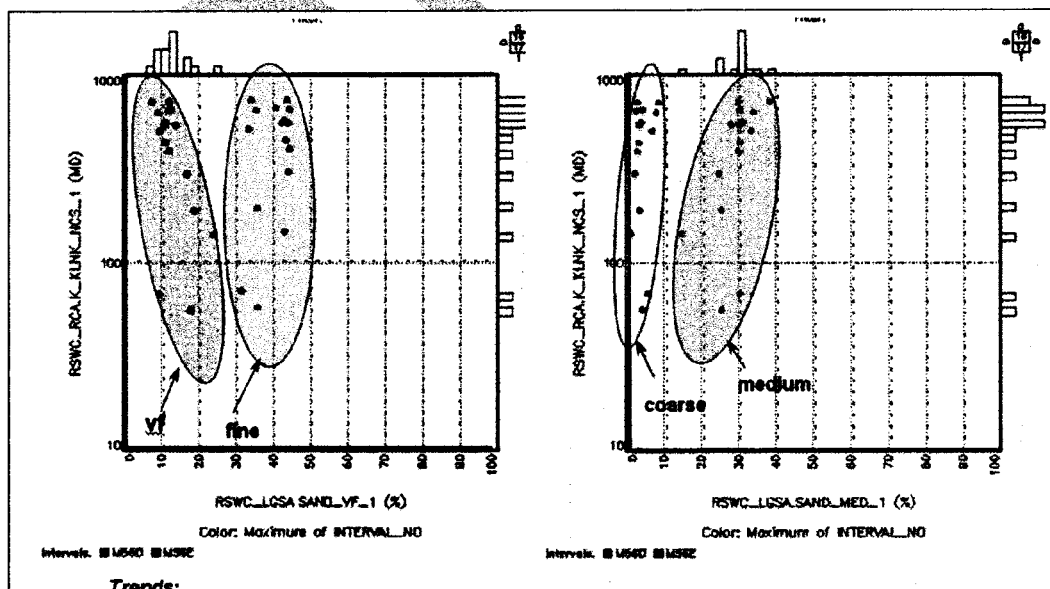


Figure 11: Laser Grain Size Analysis, Permeability vs. percentage of different (very fine, fine, medium and coarse) size sand particles.

The observations from Figures 10 and 11 leads to the suggestion that the M56E core plugs indicate slightly better sorting than the M56D plugs. This is reflected in their respective positioning in K/PHI space as indicated in Figure 12. Further the Winland iso-pore throat lines suggest that two sands may be slightly different rock types based on their degree of sorting. The 10 micron line divides the two rock type.

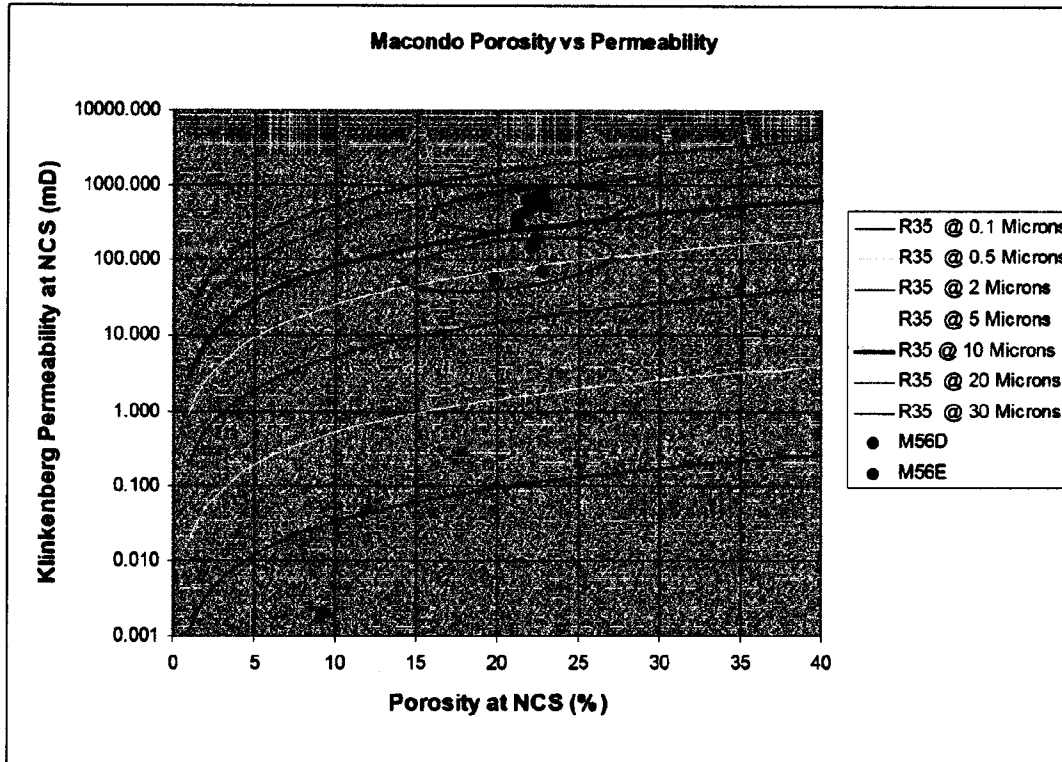


Figure 12: Winland R35 rock typing plot.

X-Ray diffraction (XRD) analysis results from 10 samples (4 in M56D and 6 in M56E) are presented in Figure 13. Mineralogical content of all analysed sandstone samples are in average 93% Quartz with Kaolinite (~2%) and Illite 1% clays, 1% K-spar and 3% Plagioclase. Based on the 10 samples from M56D and M56E there appears to be no difference in mineralogy between the two sand bodies, so any variation in petrophysical properties is likely to be a function of grain size and most likely sorting.

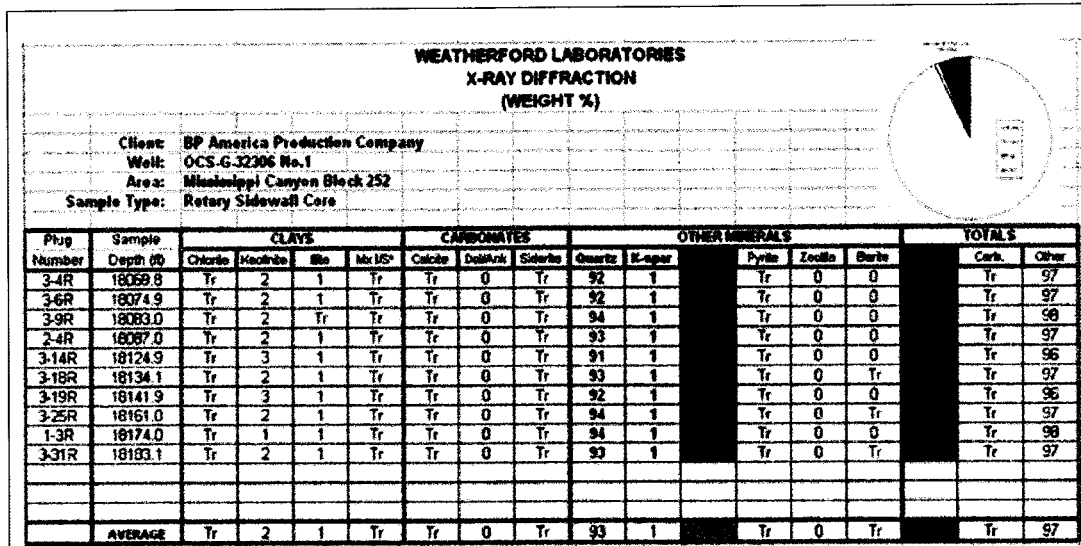


Figure 13: X-Ray Diffraction Analysis. First 4 samples (from 3-4R to 2-4R) are for M56D, 6 next samples are from M56E.

Routine Core Analysis

After the rotary sidewall core plugs were cleaned and dried, the 17 samples were subjected to Routine Core Analysis (RCA). The measurements of porosity and permeability were performed at 500 psi and at 2000 psi (NCS). The analysis also included stair steps and repeat measurements of porosity and permeability.

Klinkenberg permeability to air at NCS is plotted versus Porosity at NCS in Figure 14. M56D sand may be more heterogeneous than M56E and its reservoir characteristics are hardly described by the available samples. More core data will be necessary for rock typing work. From the Laser grain analysis - sorting may be a function in this effect more than grain size.

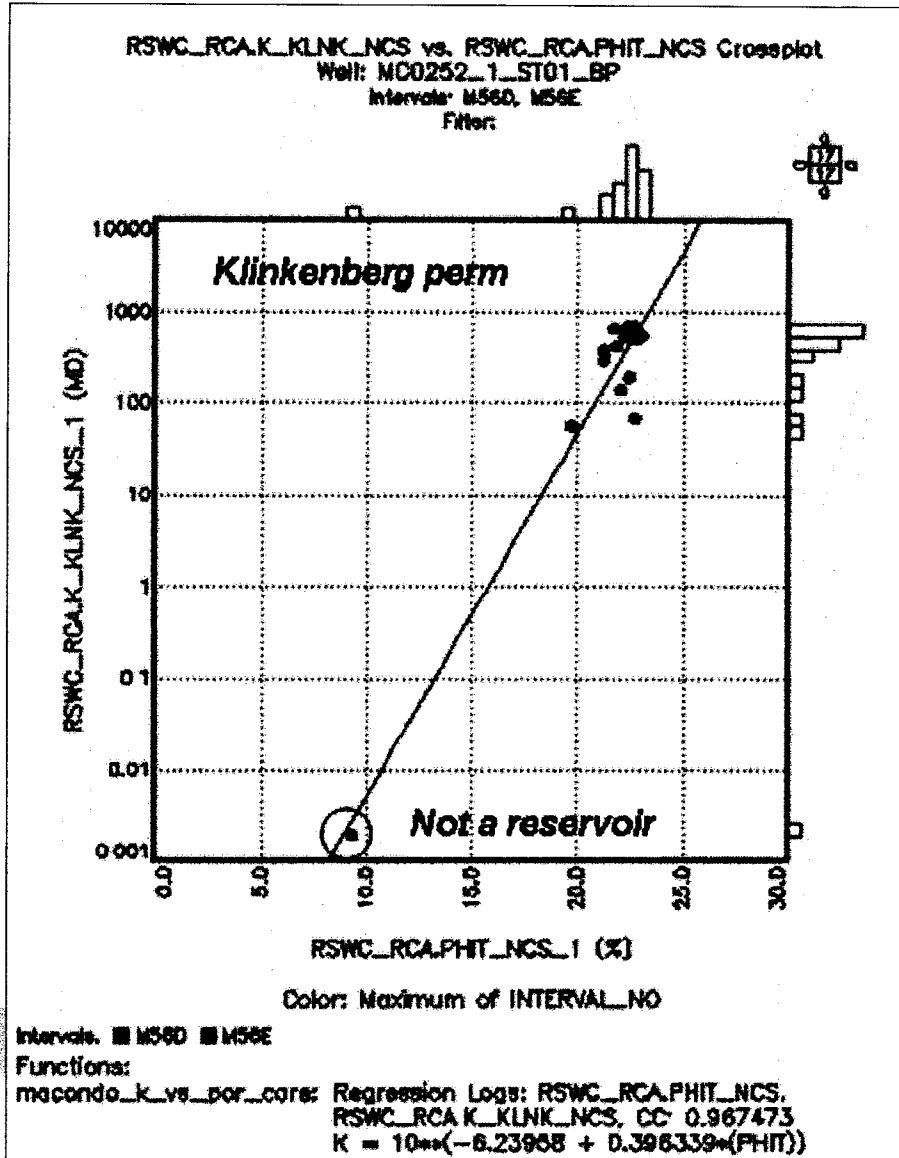


Figure 14: RCA. Klinkenberg permeability to air at NCS is plotted versus Porosity at NCS with linear regression function used for Permeability calculation.

Frequency histograms of core derived Porosity and Permeability are presented in Figure 15. Porosity of M56D samples are very close to M56E samples but Permeability is slightly less, it maybe due to sorting, packing and to grain size distribution as mineralogical content of the sands is similar.

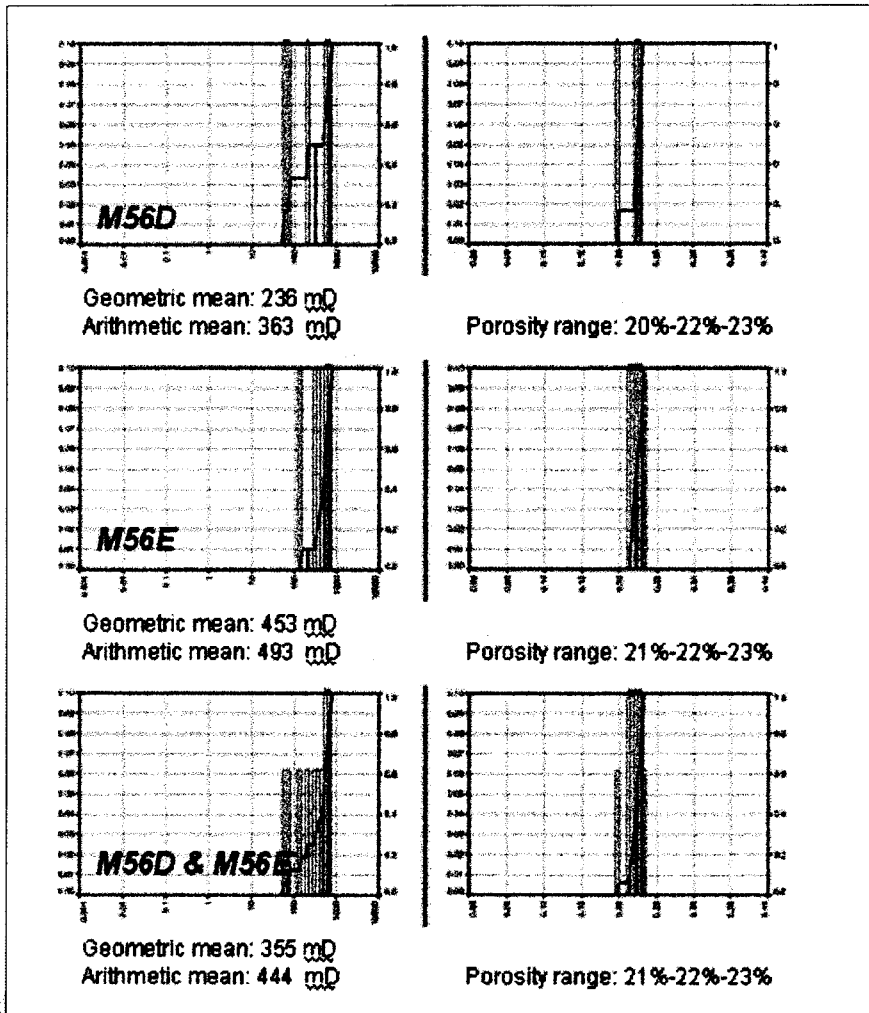


Figure 15: Frequency distribution of Core measured Klinkenberg permeability to air at NCS and Porosity at NCS separately per sands and both sands together.

Log to Core calibration

Porosity was derived from the density log from the following equation:

$$\text{Density porosity (dec)} = (\text{Rhog} - \text{Rhob}) / (\text{Rhog} - \text{Rhof})$$

- Where:
- Rhog is grain density (g/cc)
 - Rhob is the density log (g/cc)
 - Rhof is the fluid density (g/cc)

Grain Density (Rhog) and Fluid Density (Rhof) were determined from core derived data.

Frequency distributions of core measured Rhog and log Density (Rhob) vs. core measured porosity (Phit_ ncs) plot are presented in Figure 16.

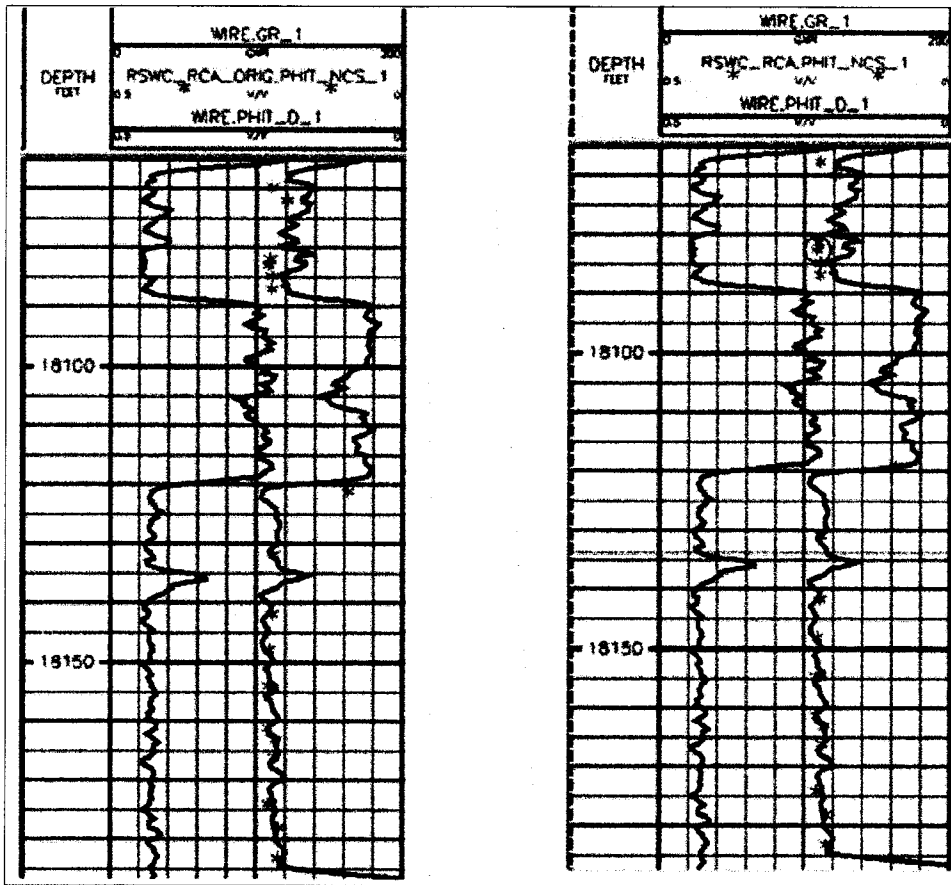


Figure 17: Calibration Logs to core. Core porosity at NCS overlays with Density log derived porosity. Original sidewall core plug depths on the left plot, depth shifted plugs on the right.

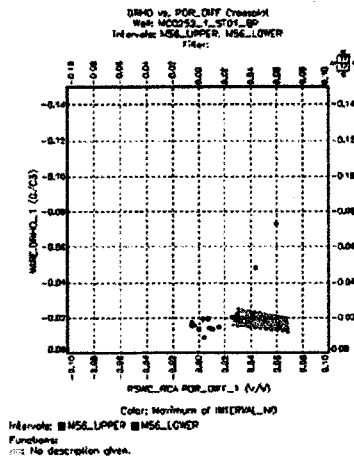
Porosity calculated from density log in upper lobe (M56D) is 2-6 porosity units lower than core derived porosity while in the lower lobe (M56E) they match well.

One of the possible reasons for this mismatch is overcorrecting of the density log (RHOB) for barite additives to mud. The degree of correction (DRHO log) is shown by the red shading in Figure 18.

On the left side in Figure 18a, DRHO (Y axis) is plotted versus the difference between core porosity and density derived porosity (X axis). For M56E sand (in blue) the difference is +/- 1 porosity unit while density correction DRHO is around -0.015 g/cc; For M56D sand (in green) the density correction and the porosity difference are higher for most of the samples.

The large DRHO corrections match spikes in the PEF curve indicating the greatest barite effect (blue curve in Neutron-Density track) in Figure 18b.

Density correction (DRHO) vs. difference between Core porosity and log porosity.



If Upper sand was affected by barite as Lower sand DRHO should be -0.015 g/cc

Density correction (DRHO) vs. difference between Core porosity and log porosity.

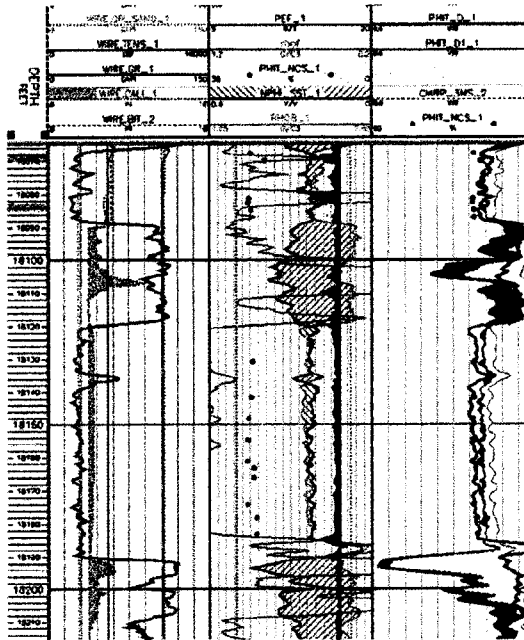


Figure 18a and Figure 18b: Density log correction in M56D.

To eliminate the over correction, DRHO values ≤ -0.015 were replaced by -0.015 and Rhob in upper sand M56D log was corrected and used for density porosity calculation.

After the correction was made, the Density porosity (Phit_Upper) matched Core porosity more closely and the extrapolated fluid density matched much closer to the fluid density of 0.845 g/cc, estimated in M56E. As the reservoir fluids in both reservoirs are very similar and the mud filtrate is the same this is a reasonable outcome (Figure 19).

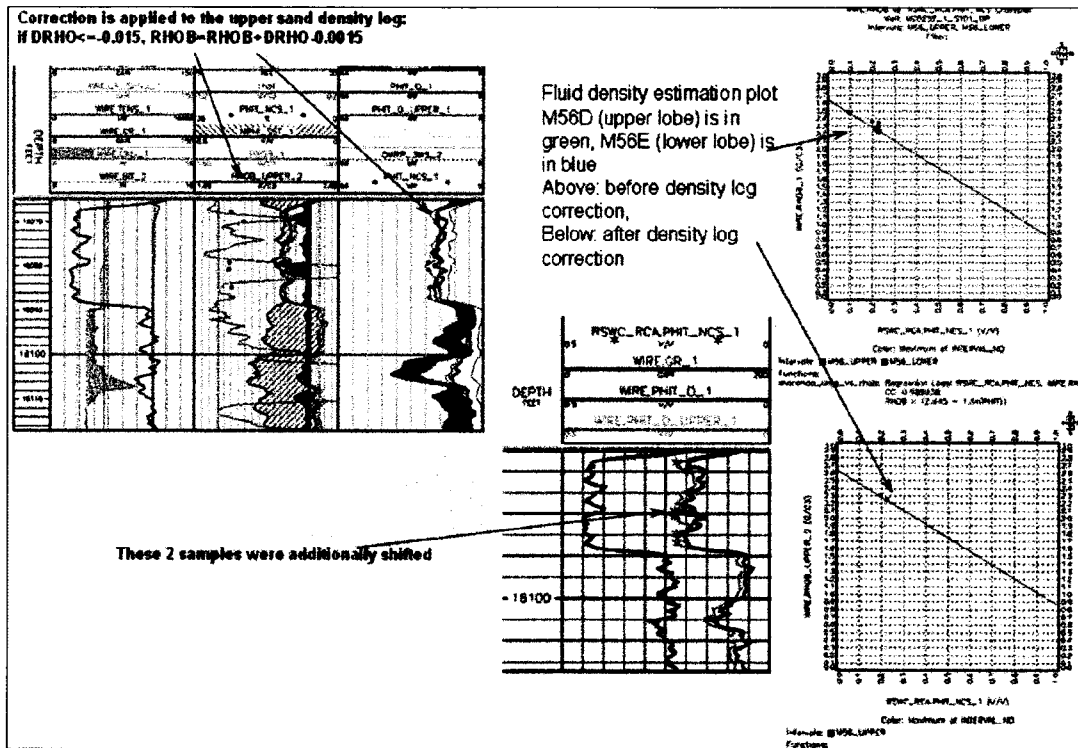


Figure 19: Overlaying Density porosity in M56D with core porosity and cross plots of corrected Density log with core porosity for Fluid density estimation.

The need to make this correction to tie the core data suggest a slightly higher uncertainty in petrophysical parameters in the M56D sand compared to the M56E sand.

There may be other factors to take in to consideration such as anisotropy due to thin beds.

Permeable intervals

Volume of shale (Vsh) cut-off was used to identify permeable intervals.

Gamma Ray log was used for Vsh estimation. For VSH calculation GR_sand and GR_shale lines were created and Vsh was derived as:

$$Vsh = \frac{GR - GR_{sand}}{GR_{shale} - GR_{sand}}$$

The sand and shale lines were adjusted to reflect the sand percentages from the mudlog and Quartz volume estimated by of ECS log.

For identifying all possibly permeable layers a Volume of shale (VSH) cut-off of 0.4 is used.

The cumulative sand count for each of the permeable sands is presented in Figure 20.

| | TOPS_SAND TYD_I | TOPS_SAND TYD55_I | TOPS_SAND FORMATION_I | TOPS_SAND LIM_GROSS_SAND |
|------------|--------------------|----------------------|--------------------------|-----------------------------|
| 17467.0000 | 17456.07351 | 17381.07351 | M57B | 2.00000 |
| 17469.0000 | 17458.07347 | 17383.07347 | | |
| 17700.0000 | 17689.07027 | 17614.07027 | M57C | 8.50000 |
| 17708.5000 | 17697.57014 | 17622.57014 | | |
| 17804.0000 | 17793.06826 | 17718.06826 | M56A | 2.50000 |
| 17806.5000 | 17795.56821 | 17720.56821 | | |
| 17975.5000 | 17964.56328 | 17889.56328 | M56B | 5.00000 |
| 17989.5000 | 17978.56256 | 17903.56256 | | |
| 18030.0000 | 18019.06017 | 17944.06017 | M56C | 2.00000 |
| 18032.0000 | 18021.06004 | 17946.06004 | | |
| 18067.0000 | 18056.05774 | 17981.05774 | M56D | 22.00000 |
| 18089.0000 | 18078.05618 | 18003.05618 | | |
| 18120.0000 | 18109.05382 | 18034.05382 | M56E | 69.50000 |
| 18191.0000 | 18180.04842 | 18105.04842 | | |
| 18217.5000 | 18206.54683 | 18131.54683 | M56F | 6.50000 |
| 18238.5000 | 18227.54573 | 18152.54573 | | |

Figure 20: Cumulative sand thickness per sand unit

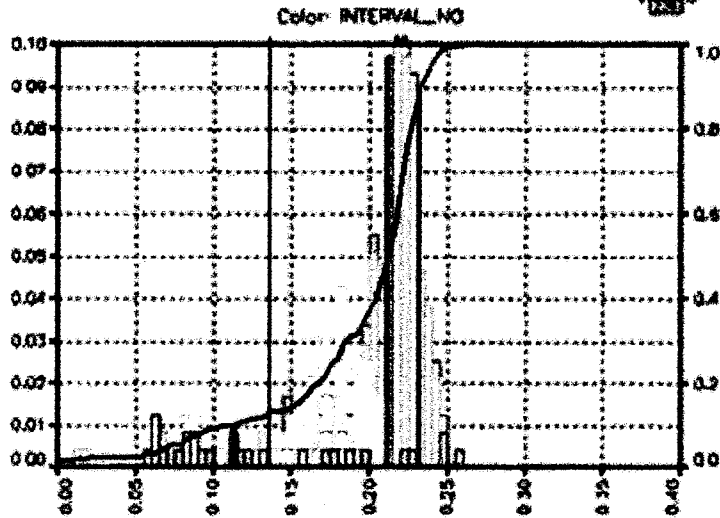
Petrophysical parameters calculations

Determination of net sand cut off

A frequency histogram of Density porosity is presented in Figure 21. A net sand cut off of 14 % porosity and < 0.4 Vsh was used. These values are based on GOM analog Middle Miocene wells. There is not enough core data to confirm these parameters with permeability distributions.

The Density porosity was compared to Core porosity in M56D and M56E sands, where rotary sided wall derived porosity was used for calibration. In spite of an apparent slight gas signature on Neutron-Density log and GMR porosity being lower than Density porosity (usual for gas sands), fluid sampling of both reservoir sands showed volatile oil, therefore no gas correction applied to the Density log. The density log derived porosity has been demonstrated to tie reasonably well to porosity from core plugs.

Histogram of WIRE_PHT_D
 Well: MCD252_1_5701_BP
 Intervals: M57B, M57C, M56A, M56B, M56C, M56D, M56E, M56F
 Filter: MDCENE_GROSS_SAND_FLAG=1



| Statistics | | Intervals | |
|--------------------|----------|------------|---------|
| Possible values | 236 | 1. M57B | |
| Missing values | 0 | 2. M57C | |
| Minimum value | -0.00672 | 3. M56A | |
| Maximum value | 0.29833 | 4. M56B | |
| Range | 0.26406 | 5. M56C | |
| Mean | 0.19109 | 6. M56D | |
| Geometric Mean | - | 7. M56E | |
| Harmonic Mean | 0.16949 | 8. M56F | |
| Variance | 0.00298 | | |
| Standard Deviation | 0.05460 | Percentage | |
| Skewness | -1.08781 | 10% | 0.11320 |
| Kurtosis | 0.98631 | 50% | 0.21167 |
| | 0.51224 | 90% | 0.23227 |

Figure 21: Density porosity histogram with 14% cut off.

Density porosity distribution in the M56E net sand was compared to Core porosity and presented in Figure 22. It shows a good match in minimum, maximum and most likely values. The same histograms for M56D did not show a good match due to underestimating the porosity in this sand if the uncorrected density is used for the calculation (Figure 23).

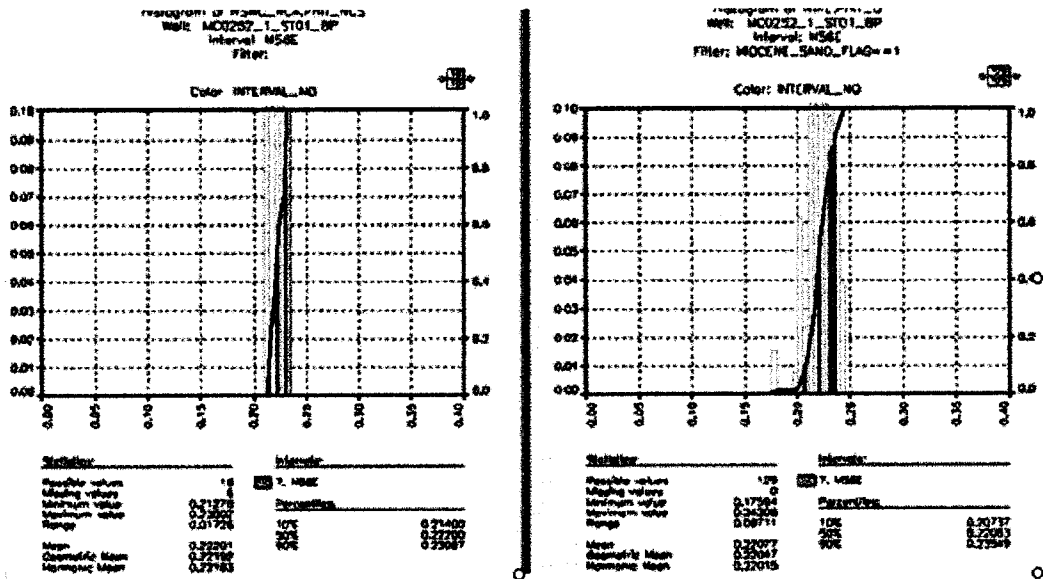


Figure 22: Density Porosity distribution in M56E sand vs. Core porosity.

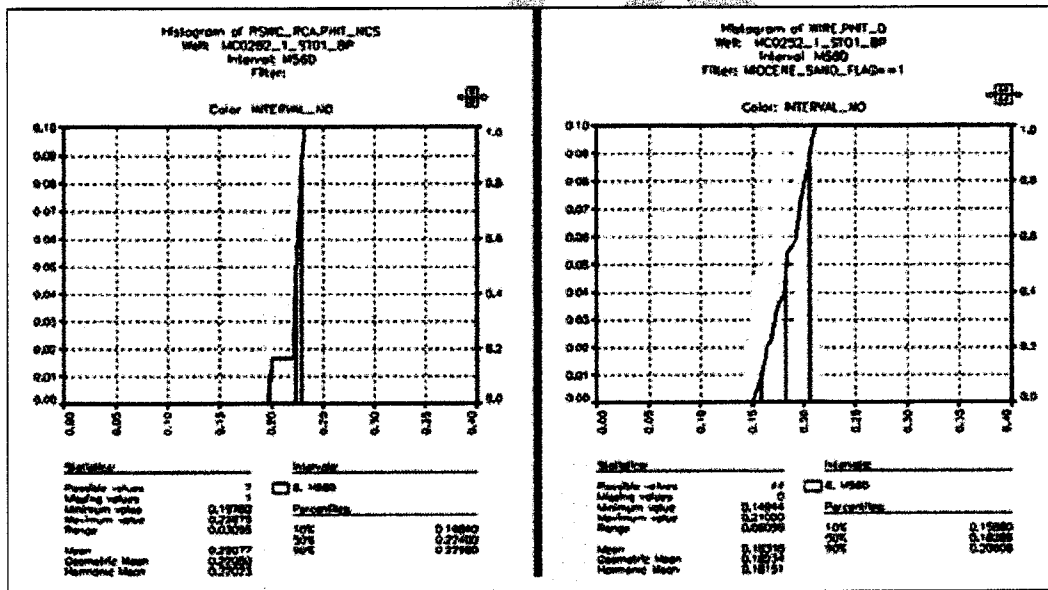


Figure 23: Density Porosity (with uncorrected density input) distribution in M56D sand vs. Core porosity.

If the corrected density is used in the M56D sand for porosity calculation the comparison with core data is closer (Figure 24).

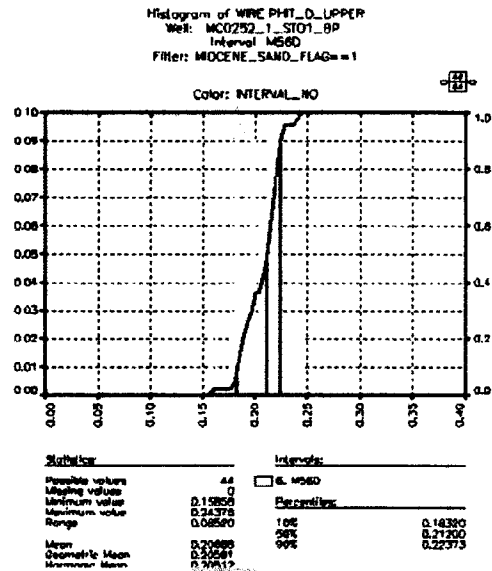
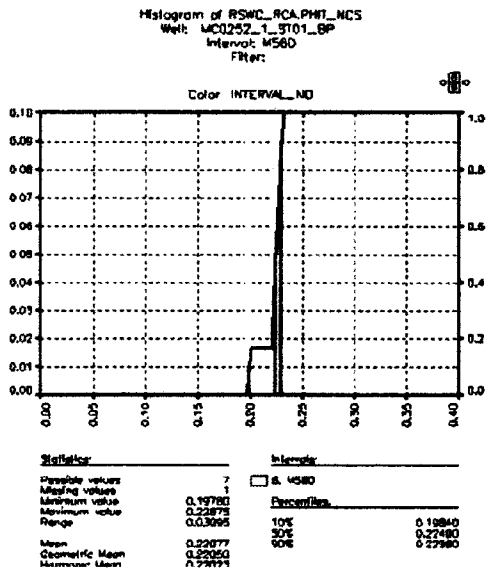


Figure 24: Density Porosity (with corrected density input) distribution in M56D sand vs. Core porosity.

Three further sands have been identified in the TD hole section, which have a gas signature on Neutron-Density logs: namely M57B, M56A and M56F. No core samples were taken in the M57B and M56A sands though one sample was taken in M56F and is currently under evaluation.

Fluid typing of the sands is uncertain and parameters are difficult to assess accurately due to the thin nature of these sands, being below confident log resolution. At this point of interpretation no gas correction applied to the Density porosity in these sands

Water Saturation (Sw)

No thick aquifer sand was observed in the interval of evaluation to determine Rwa.

An assumed regional value of R_w of 0.021 Ohmm at a bottom hole Temperature of 243°F from control data was used for Sw evaluation.

The parameters, a=1, m=1.81 and n=1.88 from the Isabella analog well were used to calculate Sw using the Archie equation.

The Sw evaluation will be re-visited after Electrical properties and Mercury Injection Capillary Pressure measurements are finished. Sw is a subject to some uncertainty currently.

Frequency histograms of Sw are presented in Figure 25. The Sw cut off for pay is estimated at 50 %. The cut off value will be revisited after SCAL results are available

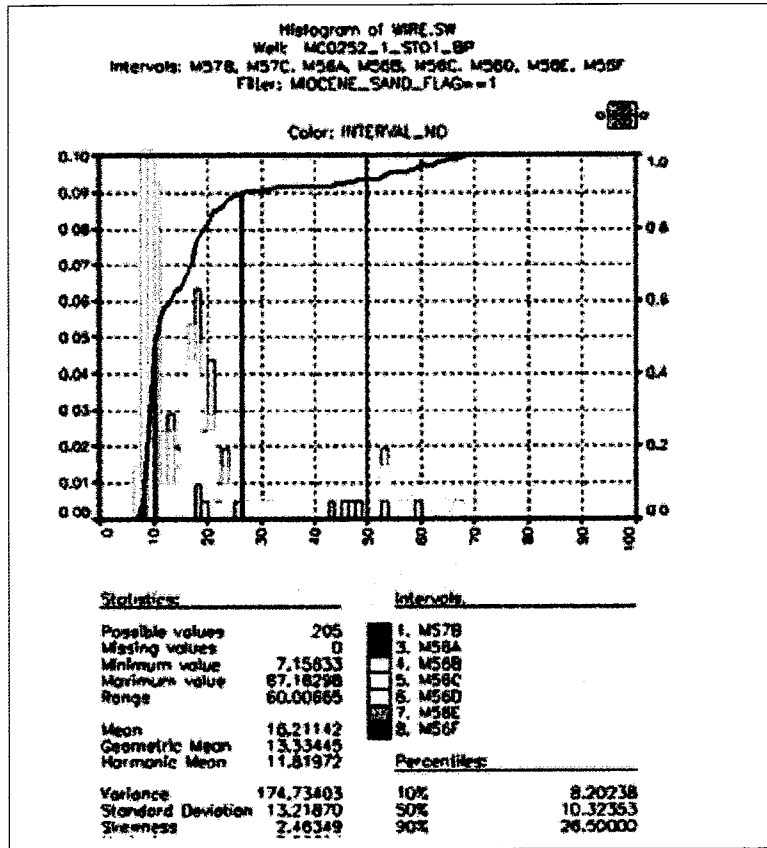


Figure 25: Water saturation Sw histogram with Sw=50% cut off.

Permeability

Permeability (to air) was calculated using core derived equation of:

$$K=10^{*(-6.23958 + 0.396339*(PHIT_D*100))}$$

Where PHIT_D is density porosity in v/v

Log derived permeability in the M56E net sand was compared to Core permeability and presented in Figure 26. It shows reasonable match in geometric and arithmetic mean values. A similar histogram for M56D did not show good match because the Permeability was calculated using Density porosity derived with uncorrected density (Figure 27).

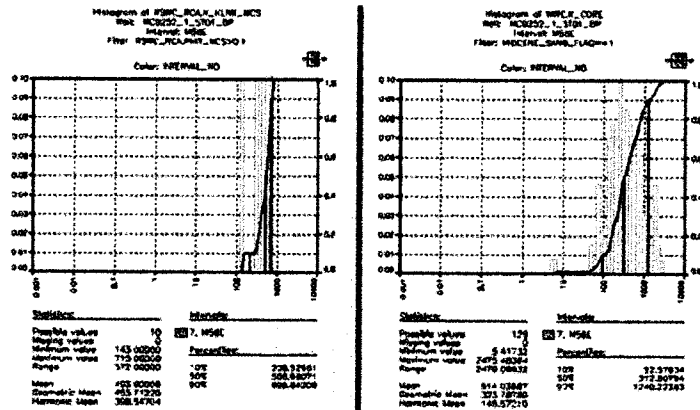


Figure 26: Log derived Permeability distribution in M56E sand vs. Core Permeability.

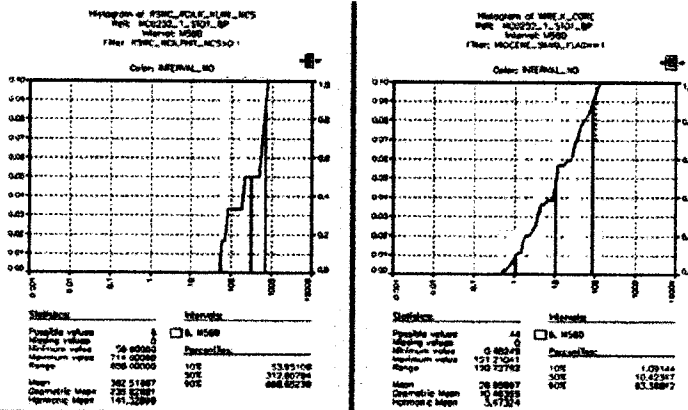


Figure 27: Log derived Permeability distribution in M56D sand vs. Core Permeability. Underestimated due to Density porosity derived with uncorrected density log input.

After using corrected density for porosity evaluation and following it Permeability evaluation, the match to Core is better, see Figure 28.

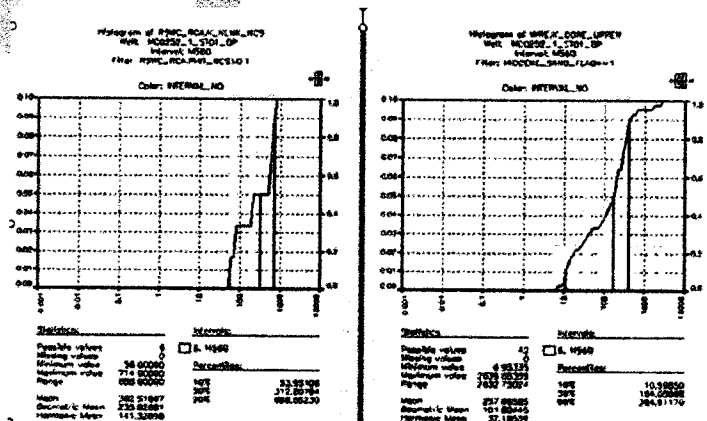


Figure 28: Log derived Permeability distribution in M56D sand vs. Core Permeability. Closer to Core Perm distribution when Density porosity derived with corrected density log input.

Fluid Typing

Based on MDT pre-test pressure data analysis and fluid sampling analysis, the M56D and M56E reservoirs comprise volatile oil with GORs of around 3000 with an API gravity of 35. A more complete set of data and analysis will be presented in Fluid Properties section.

The M56F sand underlying the main pay zone was not sampled by the MDT tool but based on its location below M56D and M56E and below the thermogenic front it is likely to be oil.

The fluid analysis of the M57D and M56A sands is uncertain (Figure 29). Sand M56A has a sonic log signature similar to M56D and M56E, which are oil bearing sands. Sonic porosity calculated in the sand matched density porosity, which also an evidence to be oil sand as Sonic porosity is usually higher than density porosity in gas sand. Based on its position on the boundary of thermogenic front – right above it, it could be gas.

The M57B sand is approximately 2 feet thick and likely to be below log resolution for accurate fluid determination, but based on its position above the thermogenic front it is likely to be gas.

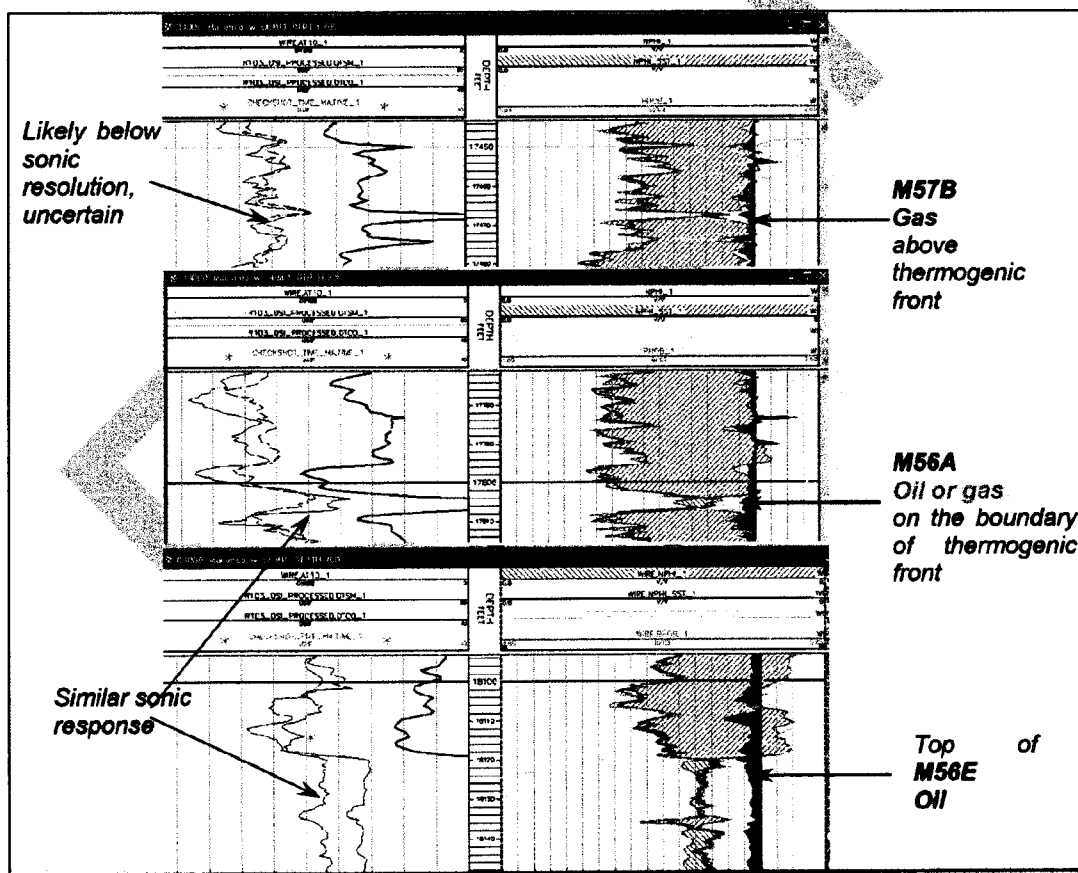


Figure 29: Fluid typing of sands M57B and M56A.

The M57C Sand was pressure tested by the LWD real time Geotap pressure tool at 17606' MD with an equivalent mud weight pressure of 14.19 ppg. This pre-test failed to repeat on re-

logging with the MDT due to repeated seal failure. The OBM image suggests that the sand is very thinly interbedded (Figure 30) and the thin sand stringers are below density log resolution so the evaluation of porosity, Sw and fluid type is compromised.

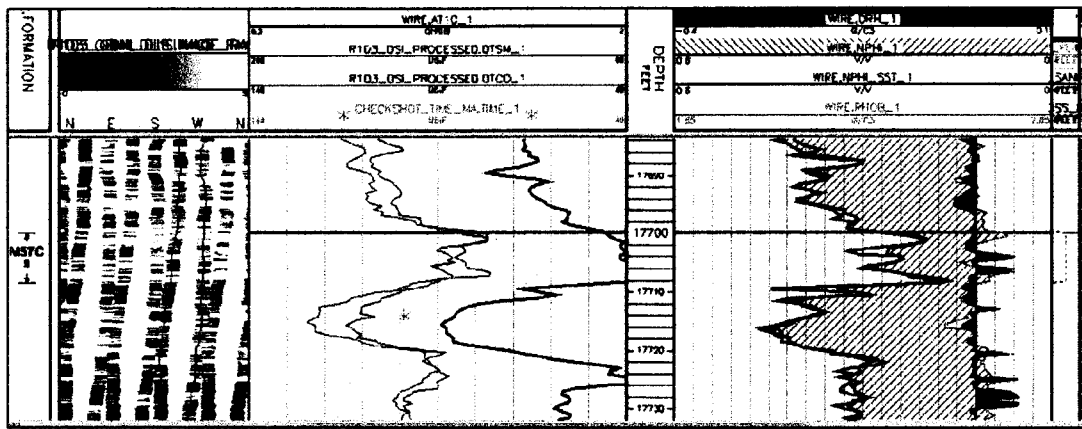


Figure 30: Logs over sand M57C.

Sands M56B and M56C are thin water bearing sands.

Reservoir and fluid quality

Despite limited core data availability, the integration of the core, log and pressure data suggests that:

- Both M56D and M56E sands have good reservoir quality and reservoir fluid.
- Based on XRD data, the M56D and M56E sand lobes have similar mineralogical content with Quartz content averaging 93% with only minor amounts of clay and secondary minerals (Figure 13).
- Sorting, grain size and sand content are the main controls on reservoir quality.
- From Core data, two rock types have been identified; M56E comprises mainly Rock type 1 and is differentiated from Rock Type 2 by improved sorting. The rock Types are also identifiable in K/Phi space with an average pore throat radius of 10 microns dividing the Rock types. The M56D sand comprises both Rock type 1 and 2. Rock type 1 maybe associated with a more homogeneous sand package, Rock Type 2 in the M56D unit may be associated with some thin bedded pay as evidenced by increased anisotropy from the tensor resistivity data and the CMR bin porosity distribution. There is a better match between core porosity and permeability in the Rock Type 1 of the M56E sand then the more heterogeneous sands of M56D and therefore less uncertainty on reservoir parameters. Thin section data will be integrated with the rest of the data when available to strengthen these assumptions.
- Mobilities from MDT pre tests confirm the two sands have high permeability in the 100's of millidarcy range.
- Figure 31 shows the permeability estimation from different data.
 Red symbols – permeability measured on core (to air),
 Brown line – permeability calculated from Density porosity using core derived equation (see underestimation of Permeability in M56D).

Red line was used for averages instead – permeability with corrected Density porosity input.
 Blue symbols – drawdown mobilities from MDT pretests,
 Green symbols – draw down mobility from MDT samples.
 Drawdown mobility is rough estimate of permeability to oil.
 Pretests mobility do not look valid to use, MDT samples mobility multiplied by 0.17 cp viscosity can be compared to Permeability to air measured on core and calculated with logs – magenta stars.

- There is a good match of log derived porosity K_CORE and CMR derived KTIM (purple curve).
- There was some initial difficulty in acquiring MDT Pressure data in the two sands. Three fluid samples were eventually taken – 1 in M56D and 2 in M56E. All 3 samples identified same fluid - volatile oil with GOR ~3000 and API=35, PVT analysis showed viscosity=0.17 cp. After the sampling, the pressure tests program was resumed.

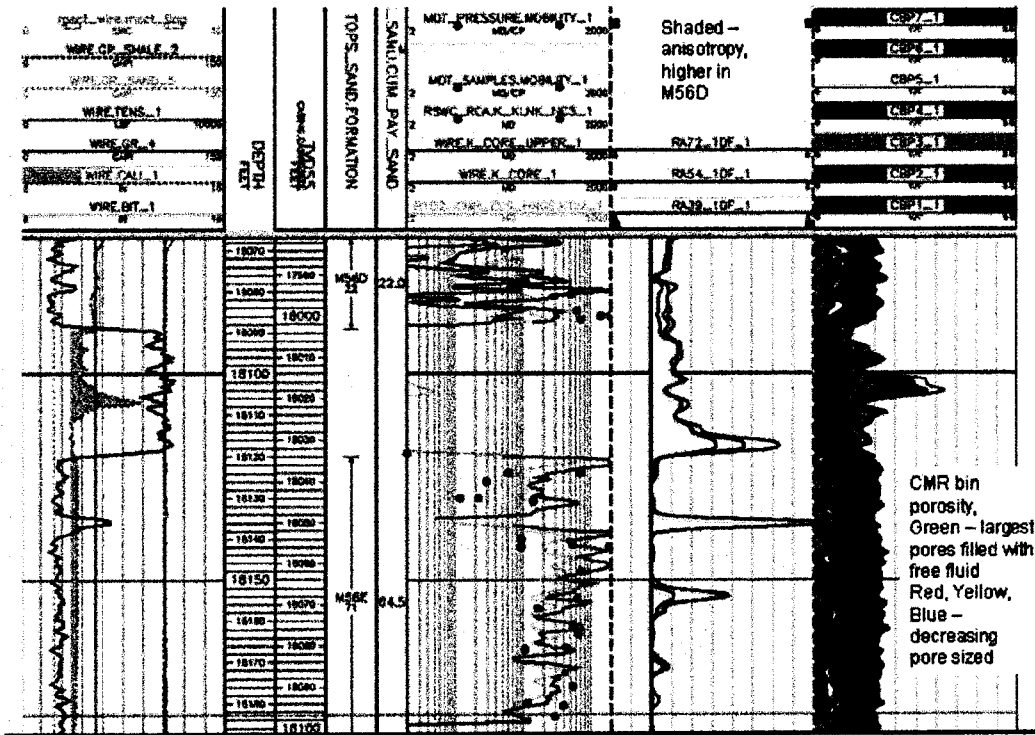


Figure 31: Logs data demonstrating M56D and M56E analysis.

- Pressure gradients are presented in Figure 32. Sample and MDT points show very slight different gradients between the two sands (0.249 psi/ft and 0.251 psi/ft for M56E and M56D respectively) but they were taken with different probes that may explain the difference.
- Water saturation uncertainty will be decreased as capillary pressure and electrical properties measurements are available.

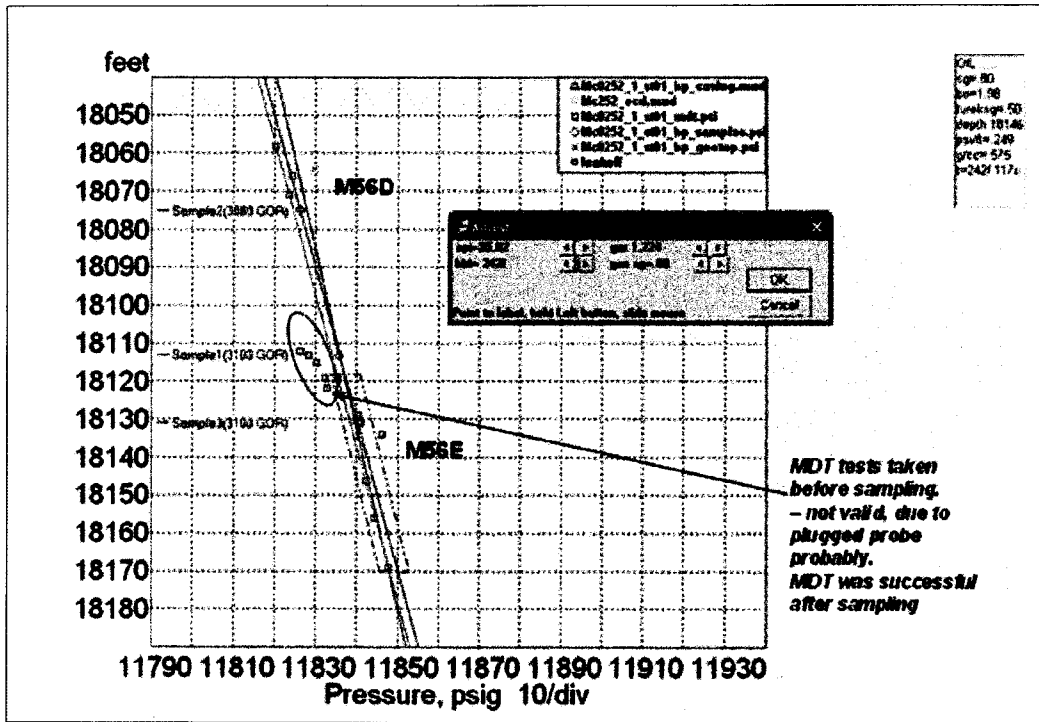


Figure 32: Presgraf pressure plot.

Net/Pay summary

Summary table is presented in Figure 33. For M56D corrected Density porosity, Sw and Permeability are used for averaging.

| Start Depth (ft) | End Depth (ft) | Start Pressure (psig) | End Pressure (psig) | Fluid Type | Formation | Porosity (%) | Sw (%) | Permeability (md) | Net Pay (ft) | Pay (ft) | Area (ac-ft) | Volume (bbl) |
|------------------|----------------|-----------------------|---------------------|------------|-----------|--------------|--------|-------------------|--------------|----------|--------------|--------------|
| 17700.0 | 17708.5 | 17614.1 | 17622.6 | Uncertain | M57C | 8.5 | 0 | 0 | 9 | | | |
| 17975.5 | 17989.5 | 17889.6 | 17903.6 | Brine | M56B | 5 | 3 | 0 | 14 | 17 | 59 | 7 |
| 18030.0 | 18032.0 | 17944.1 | 17946.1 | Brine | M56C | 2 | 2 | 0 | 17 | 17 | 64 | 5 |
| 18060.0 | 18069.0 | 17980.0 | 17988.0 | Oil | M56D | 22 | 22 | 22 | 21 | 21 | 11 | 17 |
| 18120.0 | 18121.0 | 18020.0 | 18021.0 | Oil | M56D | 20 | 20 | 20 | 20 | 20 | 18 | 10 |
| 18170.0 | 18220.0 | 18120.0 | 18170.0 | Oil | M56D | 15 | 15 | 15 | 15 | 15 | 14 | 10 |

Figure 33: Macondo net/pay summary table.

Petroleum Systems and Fluid Properties

Temperatures (pre- versus post-drill)

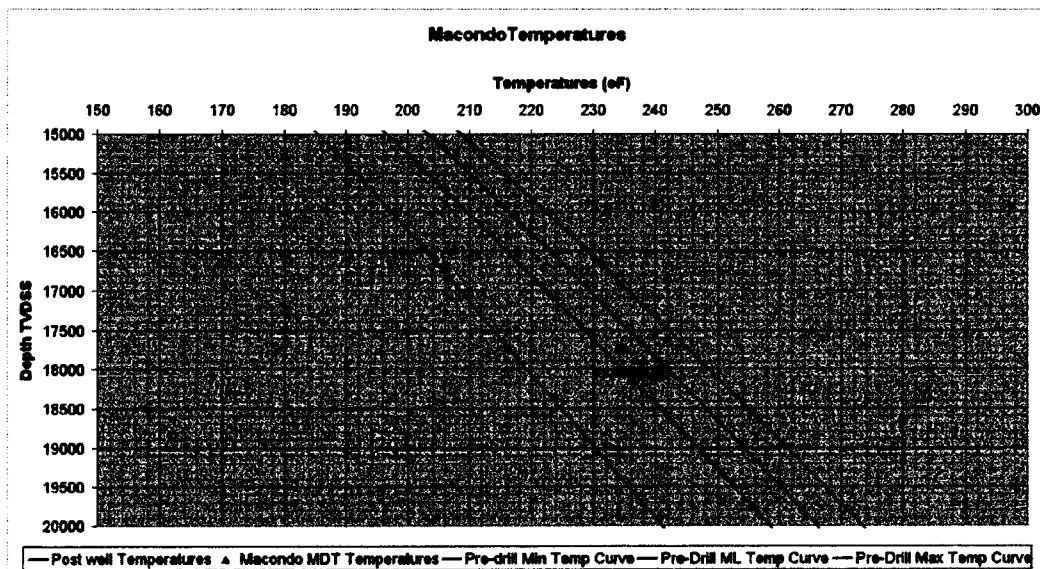


Figure 34: Pre- versus Post-drill temperature comparison.

The reservoir temperatures were predicted to be in between 219 and 248 °F, with a most likely case at 235 °F. The post well temperatures, acquired from the MDT tool gave a broad range between 230 and 242 °F (Figure 34). Therefore the post-drill temperature range was similar to the pre-drill temperature prediction.

The black curve is the post-well temperature curve. It takes into account the outer limit of the MDT temperatures as the closest reservoir temperature reading.

The post-well temperature curve is slightly above the most-likely pre-drill curve (~7 °F) but is close to the pre-drill temperature prediction. The 7 °F temperature difference should not impact the rest of the subsurface work.

Headspace & Isotope (Reservoir zone)

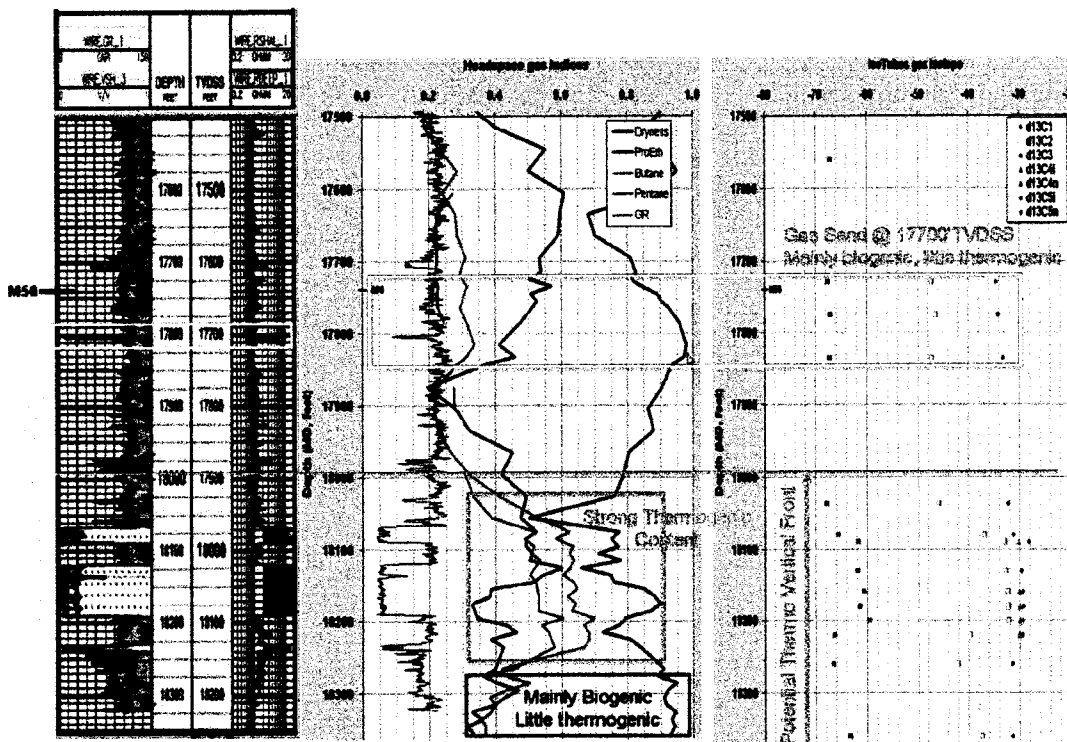


Figure 35: headspace gas indices and isotope results from isotubes.

Using the headspace gas indices and isotope results from isotubes, the thermogenic vertical front appears at 18000' MD (17900' TVDSS) (Figure 35). Indeed, the pro-ethane, butane, and pentane indices increase drastically, while the dryness index severely decreases. Moreover, the methane isotopes appear less depleted and the butane isotopes become present.

The base of the well (below 18250' MD / 18150' TVDSS) has more a biogenic signature. It is believed that the vertical thermogenic front does not pass exactly by the wellbore, giving the idea of a lateral charge. However, it is certainly a vertical thermogenic front.

The section shallower than 18000' MD (~17900' TVDSS) has a strong biogenic signature with some rare amount of thermogenic hydrocarbon. However, it is mainly biogenic gas. The sand at 17800' MD (17700' TVDSS) is a good example: it is mainly biogenic methane, but has a small amount of ethane and propane coming from the thermogenic charge. This charge was lateral in nature.

Fluid properties

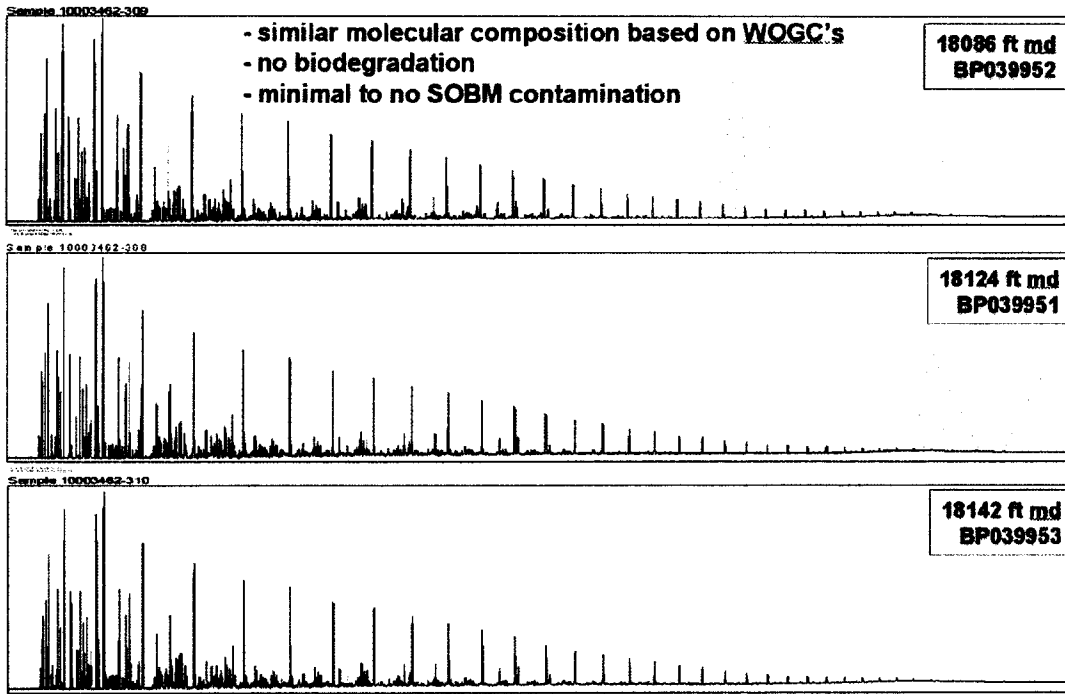


Figure 36: Chromatograms for the three dead oil samples derived from the 3 fluid samples.

Three fluid samples were taken at the level of the reservoir zone: one sample in the M56D sand (upper sand lobe at 18086' MD / 17999' TVDSS), and 2 samples in the M56E sand (middle sand lobe at 18124' and 18142' MD / 18037' and 18055' TVDSS).

Three dead oil samples were derived from those 3 fluid samples and were analysed for whole gas chromatography. The chromatograms are shown in the Figure 36.

By comparing the three chromatograms, we can conclude that the 3 oil samples have a very similar molecular composition, that there is no biodegradation and a minimal contamination level from the drilling mud.

By looking at the headspace and isotube concentrations as well as the isotope signatures, we can also conclude that the M56D, M56E, and M56F sands are oil and have similar composition. The M56F sand (18250' MD) is oil but has a higher content of biogenic gas than the M56D and M56E sands.

MDT fluid samples were taken at three depths. These are the volumes that were obtained during sampling.

| Sample Depth | 2 ¾ gallons | MPSR | SPMC |
|--------------|-------------|------|------|
| 18086' MD | 1 | 4 | 2 |
| 18124' MD | 1 | 4 | 2 |
| 18142' MD | 1 | 6 | 0 |

The three samples were tested offshore for quality assurance. The results from a single flash are summarized below.

| Sample Depth | Contamination | Gas-Liquid Ratio (scf/stb) | Liquid API | Gas Gravity | Reservoir Pressure (psi) | Temperature (F) |
|--------------|---------------|----------------------------|------------|-------------|--------------------------|-----------------|
| 18086' MD | 1.2 wt % | 3017 | 34.9 | 0.7823 | 11841.04 | 241.9 |
| 18124' MD | <1.0 wt % | 2909 | 34.7 | 0.8050 | 11850.41 | 242.3 |
| 18142' MD | <1.0 wt % | 2840 | 35.0 | 0.7837 | 11855.83 | 242.6 |

After samples were brought back to shore, the MPSRs were restored for 5 days to reservoir pressure and temperature.

From flash liquid composition all three zones are the same (Figure 37).

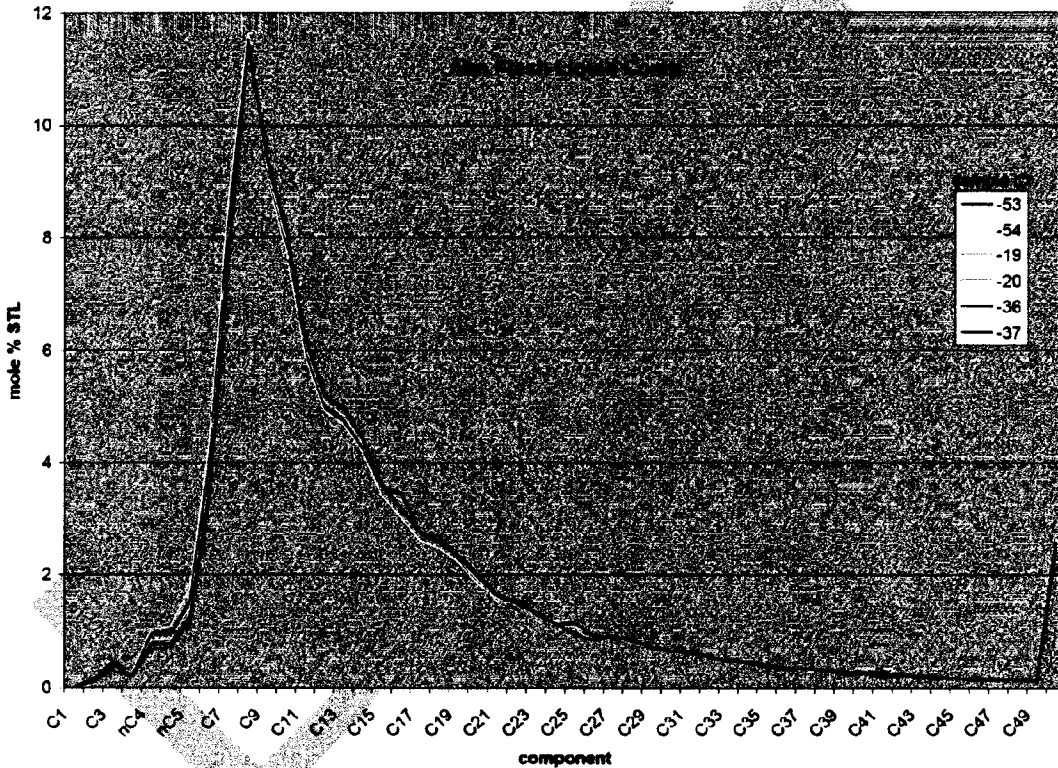


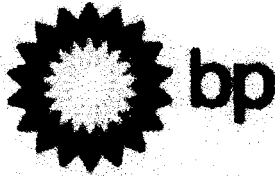
Figure 37: Flash liquid composition comparison.

Pencor conducted the initial test of the fluid at 18142' MD. The saturation pressure was determined to be 6504 psi. The liquid volume percent increased below the saturation pressure which makes it a dewpoint system instead of a bubblepoint system. From LFA records during MDT sampling it was determined this was an oil system. Therefore we had an MPSR sample sent to a separate lab, Schlumberger Oilphase, to confirm or deny the system and saturation pressure. Oilphase had a saturation pressure of 6348 psi and saw liquid volume decrease below the saturation pressure making it a bubblepoint system. A third lab, Westport, was selected to confirm the bubblepoint system. Their analysis determined it is a bubblepoint system and the saturation pressure is 6438 psi. Below is a summary of the analyses conducted by the labs for sample at 18142' MD thus far on May 24, 2010.

| Lab | Pencor | OilPhase | Westport | Comments |
|---------------------------------------|--------|----------|----------|------------------|
| Psat (psia) | 6504 | 6348 | 6438 | 18142' MD sample |
| Oil Density (gm/cc) @ Res Cond | 0.587 | 0.590 | | 18142' MD sample |
| Co (10 ⁻⁸ /psi) @ Res Cond | | 12.2 | | 18142' MD sample |
| Oil Viscosity @ Res Cond | 0.168 | | | 18142' MD sample |
| FVF (rb/stb) | 2.564 | | | 18142' MD sample |
| WAT (°F) | 89 | | | Dead Oil |

Draft





Technical Note

Title: Macondo SIWHP and Build-up Times
Prepared by: Mike Levitan, Debbie Kercho, Farah Saidi, Simon Bishop, Tony Liao, Thomas von Schroeter, Kelly McAughan, Chris Cecil
Issued by: Debbie Kercho and Chris Cecil
Date: May 26, 2010
Revision: D (Draft for Discussion)

Question Addressed in this Technical Note

As BP is currently evaluating kill options for the Macondo well, this technical report addresses the following question:

What is the estimated shut-in pressure character for the well addressing:

- a) time for Pressure Build Up at normal SIWHP
- b) ultimate shut-in pressure taking into account both the oil bearing and gas bearing sands?

Incorporation of Subsequent Work

Subsequent to forming the evaluation team for this report, a larger team was established to evaluate both the range of shut-in pressures and the probability distribution for the pressures within that range. Portions of that team's work are included in Rev. D of this text. The larger team's work is documented in a separate note: Macondo Technical Note – Shut-in Pressures: Range and Likelihood.

Key Conclusions

- 1) The SIWHP is expected to be between 7,959 psia and 8,515 psia for the various oil sands between depths of 18,067' and 18,238.5' (MD-RKB). This range is based upon measured PVT data* and assumes no significant reservoir depletion.

*Note: oil-only cases were considered using a hypothetically assumed 7,500 scf/stb GOR oil which could be consistent with a 7,475 scf/stb value reportedly observed on the Enterprise vessel during a 3-1/2 hour flow period. This GOR measurement is considered highly uncertain for a number of reasons. The case was evaluated for completeness and resulted in SIWHP between 9,450 psia and 9,600 psia.

- 2) Depending upon how much free gas from the various gas sands between depths of 17,467' and 17,806.5' (MD-RKB) is considered to be adding to the total flow, the maximum SIWHP could range between 7,515 psia and 8,615 psia. Methane was used for the dry gas PVT properties. Varying degrees of gas sand depletion were considered, as was cross-flow between oil and gas sands during the shut-in period.
- 3) Were the entire well bore to be gas filled, SIWHP would range between 9,190 psia and 11,327 psia. For this to occur it is necessary to assume that the oil sands do not contribute to flow. Finger-printing of the oil on the surface of the Gulf of Mexico confirm M56 as their source, making this assumption impossible. Methane was used for the dry gas PVT properties.
- 4) The time required for oil sands between depths 18,067' and 18,238.5' (MD-RKB) to build-up to a static SIWHP depends on the assumed location of the flow restriction.
 - a. for a case in which there is a flow restriction at a shallow location in the well the time to build-up to a nearly-static SIWHP is on the order of 5 minutes.
 - b. for a case in which there is a flow restriction located deep in the well the time to build-up to a nearly-static SIWHP is on the order of 30 minutes.
- 5) When both the gas sand at a top depth of 17,804' (MD-RKB) and the oil sands between depths 18,067' and 18,238.5' (MD-RKB) contribute to flow, the time required to build-up to a static SIWHP is essentially the same as the cases listed above in conclusions (4) a. and (4) b.

- 6) Reservoir pressure depletion is expected to range from 40 psi (assuming a production rate of 5,000 bopd) to 400* psi (assuming a production rate of 60,000 bopd) from April 20 to May 14, 2010. Such depletion would reduce all SIWHP estimates by an equivalent amount, except those calculated using the GAP software program which already includes the impact of depletion.

*Note: Reported wellhead pressure was 3800 psig initially and 3100 psig on May 14. A case was developed to determine that an initial flow rate of ~93 mbopd would be required to create sufficient reservoir depletion to account for the observed 700 psi decrease in flowing wellhead pressure using current estimates of OOIP. A new wellhead pressure of 3500 psig was reported on May 21, so this scenario is no longer considered valid.

Discussion

Shut-in Wellhead Pressure (SIWHP) – BP Estimates

All oil SIWHP calculations are based on a static formation pressure measured by MDT (11,850 psia at 18,124' MD-RKB) and PVT lab analyses from Pencor and Schlumberger. The PVT lab analyses were conducted on MDT samples taken at 18,142' MD-RKB. We have conducted QA/QC on the samples and are satisfied that they represent the reservoir fluid. The two vendors' results are consistent with each other with respect to a single phase fluid. Tests are ongoing as of May 14, 2010 on two additional samples taken at depths: 18,086' MD-RKB and 18,142' MD-RKB.

Black-Oil PVT tables were generated in Petroleum Experts software using published correlations. Initial estimates were based on reference values of Oil Gravity (35 °API,) GOR (3,000 scf/stb,) Pbp (6,650 psig,) Reservoir Temperature (240 °F,) initial Reservoir Pressure (11,850 psig) and used the Lasater correlation. The reference values were updated during the evaluation process as new data were obtained. The SIWHP values in the table below which were generated using the PROSPER and GAP software programs are generally based on the Al-Marhoun correlation using reference values of Oil Gravity (35 °API,) GOR (2,920 scf/stb,) Pbp (6,500 psig,) Reservoir Temperature (243 °F,) initial Reservoir Pressure (11,850 psig.) This correlation provided the closest match to lab-measured fluid density.

Note: Pbp = 6,650 psia is an early value obtained from the GoM Exploration team (who received it verbally from PENCOR) and has been carried through these calculations. An observed value of 6,550 psia was reported by PENCOR on Monday, April 26, 2010. More recently (May 13, 2010) values were reported by Schlumberger (-6,322 psia) and Pencor (6,504 psia:) both from CCVE tests on a sample taken at 18,142' MDRKB. In an e-mail dated May 17, 2010, Kelly McAughan stated that she is using values of 6,504 and 6,307 (no units given.)

Gas was represented as nearly-pure Methane with gas gravity of 0.554.

A complete table of SIWHP calculation methods and results follows:

| | | | | | |
|-------------------------------|---------------|------------------|---------|----------------|------------|
| M56F Zone Only | 7,959 | | | EoS Tables | Geothermal |
| M56E Oil, GOR ~3000 SCF/stb | 8,164 | | Pipesim | EoS Tables | Geothermal |
| M56F Oil, GOR ~3000 SCF/stb | 8,169 | | Pipesim | EoS Tables | Geothermal |
| M56D Oil, GOR ~3000 SCF/stb | 8,181 | | Pipesim | EoS Tables | Geothermal |
| M56D Zone Only | 8,213 | | | EoS Tables | Geothermal |
| M56E Zone Only | 8,238 | | | EoS Tables | Geothermal |
| M56e d.f. GOR ~3000 SCF/stb | 8,351 | 3 Sands | | | Geothermal |
| Zone 56DEF assumed 10mbd rate | 8,385 | | GAP | | Geothermal |
| M56A Oil, GOR ~3000 SCF/stb | 8,481 | 1 sand | Pipesim | EoS Tables | Geothermal |
| M56A Zone as oil | 8,510 | | | EoS Tables | Geothermal |
| Zone 56DEF; 10mbd; + aquifer | 8,515 | | GAP | | Geothermal |
| M56E Oil | 8,232 - 8,860 | | | Incompressible | none |
| | 9,450 | | | | Geothermal |
| | 9,600 | 1 sand | Pipesim | EoS Tables | Geothermal |
| | 7,515 | | GAP | | Geothermal |
| | 8,415 | | GAP | | Geothermal |
| | 8,503 | All 5 sands open | | | Geothermal |
| | 8,605 | All 5 sands open | | | Geothermal |
| | 8,815 | | GAP | | Geothermal |
| | 9,190 | | | EoS Tables | Geothermal |
| | 10,013 | | | EoS Tables | Geothermal |
| | 10,200 | | | | linear |
| | 10,372 | Single sand | | | Geothermal |
| | 10,569 | | Pipesim | EoS Tables | Geothermal |
| | 10,797 | 2 sands | | | Geothermal |
| | 11,184 | 1 sand | | | Geothermal |
| | 11,327 | | Pipesim | EoS Tables | Geothermal |
| | 11,363 | | | | linear |
| Legend: | | | | | |
| Oil, 3000 GOR | | | GAP | | |
| | | | | EoS Tables | |
| | | | Pipesim | | |

One further case should be noted, the only fully compositional oil simulation performed for this evaluation. IT predicted a SIWHP of 8,400 psia and was calculated using the OLGA v5.3 compositional, transient model (Ole Rygg, add energy, May 13, 2010)

Shut-in Wellhead Pressure (SIWHP) – U.S. National Laboratories Estimates

Teams from Lawrence Livermore, Los Alamos and Sandia National Laboratories provided estimates of SIWHP which range from 8,540 psia for oil alone to 9,510 psia for only gas. Methods and assumptions varied considerably between the 3 labs and are summarized by the following table, which is taken from Table 1 their report titled "Tri-Lab Calculations on Oil Pressure – Report to BP" and dated May 22, 2010.

Table 1. – Static Shut-In pressure predicted at the Well Head

| Analysis | BP | BP | BP |
|-------------|--|---|---|
| Description | Hydraulic head analysis using PVT data supplied by BP in file 32126 <i>Preliminary Data.xl</i> . | Hydraulic analysis using PVT data supplied by BP | Hydraulic analysis using PVT data supplied by BP. No separate methane (as above bubble point) |
| Assumptions | Bracketing calculations for liquid and vapor | Used column-averaged liquid oil density, no gas | Used BP provided PVT fluid properties. |
| Properties | 13,000 ft elevation change Black Oil 587 kg/m ³ Vapor Density 415 kg/m ³ | Black Oil 31 lb/ft ³ (497 kg/m ³) 13293 ft elevation change | Density will change with temperature |
| Results | 8540 psia using oil 9510 psia using gas | 8938 psia | <u>Pure BP PVT fluid:</u> 9082 psia (at equilibrium with geothermal gradient); 9187 psia (initially isothermal) <u>Pure methane:</u> 8095 psia (equilibrium); 8648 psia (isothermal) |
| Comments | Pressures consistently above 6650 psia, so fluid single phase | This represents a final steady-state condition. Initial transient shut-in pressure may be significantly higher. | SINDA/FLUINT model, 50m vertical resolution, coupled fluid/thermal solution |

Note: during the initial presentation from the National Labs, BP requested verification that the shut-in pressures would actually be lower with Methane filling the well bore than they would with the oil/gas mixture. The presenter verified that the numbers stated correctly reflect his findings. This is not consistent with BP's mental model.

The National Labs teams expressed concerns about gas bubbling to the top of the well bore after shut-in, and asked whether BP models allow for that; and also for gas re-dissolving in the oil? They believe that it could add ~200 psi and will model it if requested. Their modeling does not currently account for this.

Note: this requires confirmation with the OLGA modelers, but other team members believe that the OLGA models both account for the gas bubbling upward effect; and that the compositional OLGA model accounts for the gas re-dissolution effect.

Pressure Build-up Time

The reservoir pressure transient calculations were performed using the PIE pressure transient analysis software. Two reservoir models were used:

1) a single oil layer ($k_o = 300\text{mD}$, $h = 88\text{ft}$, $A = 3,500' \times 8,000'$, $\phi = 21\%$, $S_w = 12.3\%$, $c_o = 14.6 \mu\text{sips}$, $\mu_o = 0.168 \text{ cP}$, $B_o = 2.77\text{rb/stb}$, $P_{ri} = 11,850 \text{ psia}$)

2) two layers, the first identical to the previously described oil layer and the 2nd mimicking a gas layer which has the same areal extent, water saturation and porosity, $h = 3\text{ft}$, $k_g = 15 \text{ mD}$ (equiv. $k_o = 72\text{mD}$) and $P_{ri} = 12,028 \text{ psia}$. This model incorporates cross-flow between the two layers in the well bore. The initial model date was May 3, 2010.

Rates of 5,000 bopd and 25,000 bopd were assumed for the flow period in these calculations. There was no significant difference in the build-up times between cases using these assumed flow rates.

The well bore portion of the pressure calculations were performed using OLGA software with the bottom-hole pressure calculations from PIE as a boundary condition.

Reservoir Depletion

Reservoir pressure depletion due to production was evaluated using the MBal software. Model inputs included: 11,850 psig initial reservoir pressure, 188 mmstb original oil in place (based on volumetric calculations,) no aquifer, no gas cap, $S_w = 15\%$, $c_f = 6 \mu\text{sips}$, $c_w = 4.5 \mu\text{sips}$; Corey exponents and endpoints of 1.2 and 0.63 for water, 2 and 0.8 for oil, 1.5 and 0.9 for gas.

Three production rate scenarios were evaluated. A wellhead restriction was added to restrict initial rate to 5, 20 and 60 mbopd. The production rate was allowed to decrease as reservoir pressure depleted. For the time period from April 20 – May 15, 2010, the expected depletion is 40 psi for the 5 mbopd case and 460 psi for the 60 mbopd case.

Further MBal work was performed to determine what withdrawal rate would have been necessary for reservoir depletion alone to account for the reported 700 psi decrease in flowing well head pressure from the value of ~3,800 psig measured on May 8, 2010 to the value of ~3,100 psig measured on May 15, 2010. Modelling showed that an initial rate of ~93 mbopd would be necessary to cause sufficient depletion to create this

pressure response. This model assumed the same reservoir parameters as listed for the 40 – 460 psi depletion cases. A new wellhead pressure of 3,500 psig was reported on May 21, 2010, so this scenario is no longer considered relevant.

DRAFT

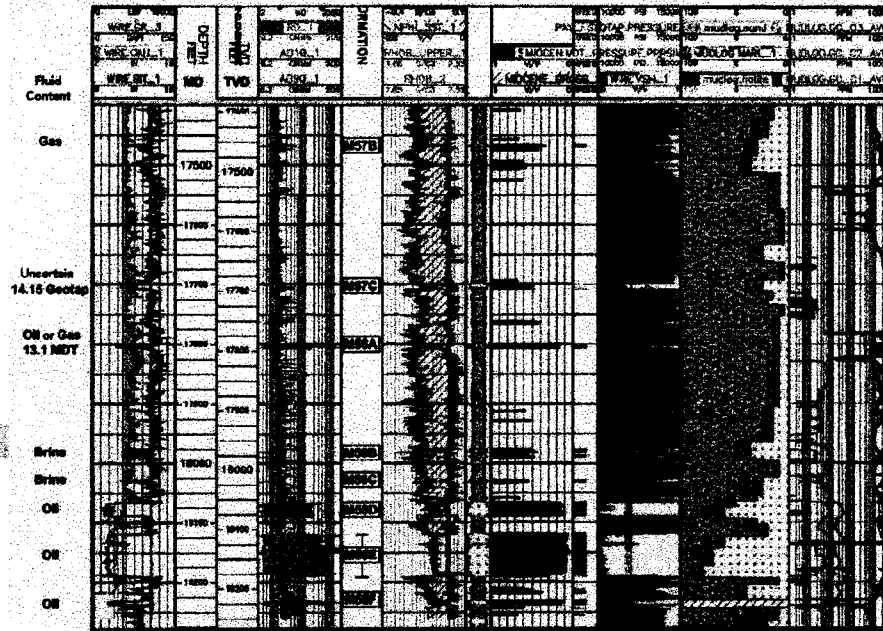
Appendix

Reservoir Description

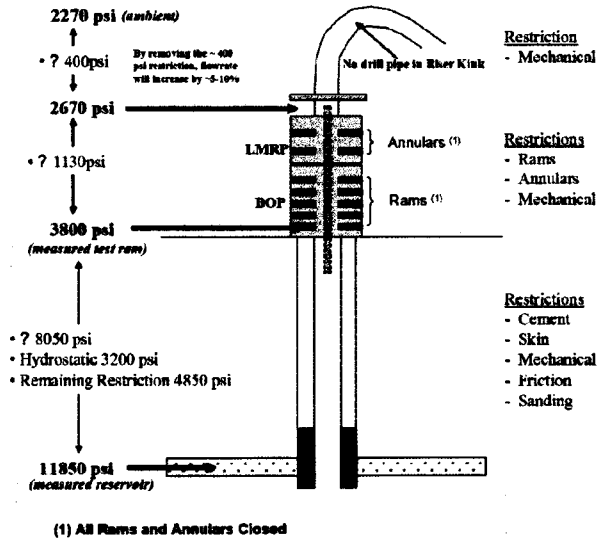
Macondo Sand Identification

5/18/2010

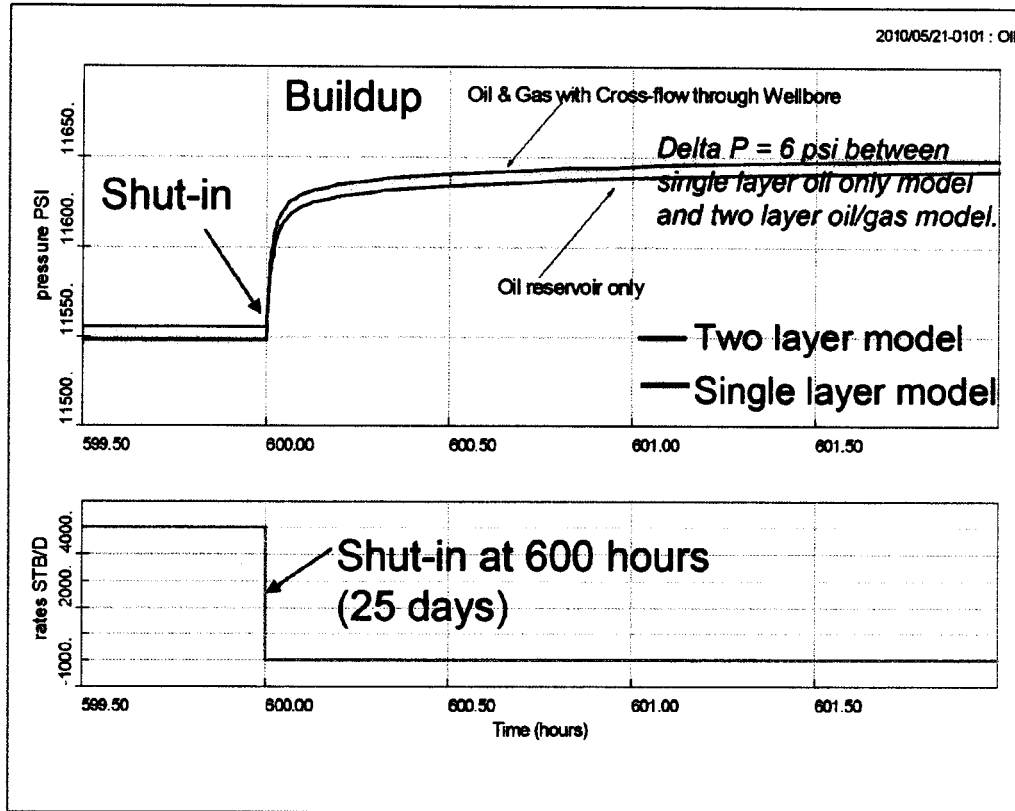
Gulf of Mexico SPU



Current Available Pressure Measurements and Well Conditions



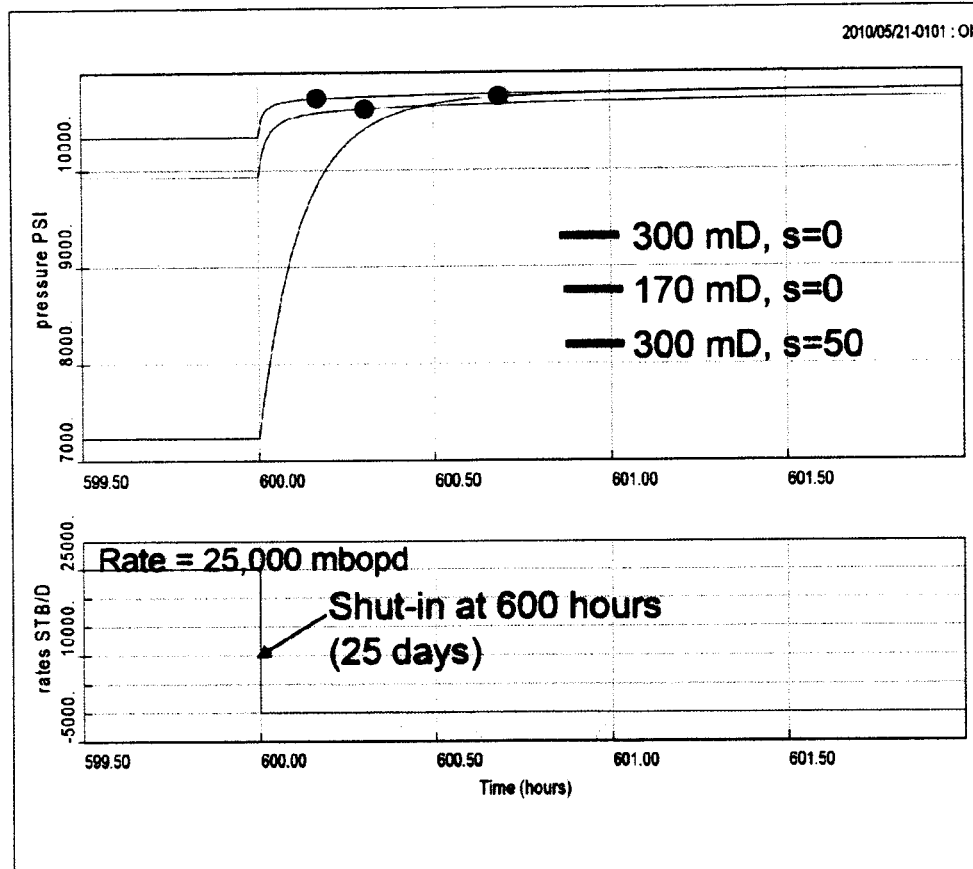
Comparison of Single Layer Oil and Two Layer Oil & Gas Reservoir Pressure Build-up Cases



Two-layer Reservoir with NO Cross-flow and Limits

| | | | |
|------------------------------|-------------------|-------------------------------------|--------------------|
| ** Simulation Data ** | | <u>Type-Curve Model Static-Data</u> | |
| well. storage = | 0.10000 HBLS/PSI | 'wall' thick. = | 0. FEET |
| Skin(1) = | 0. | Layer-1 Thick. = | 3.00 FEET |
| Skin(2) = | 0. | Layer-2 Thick. = | 88.0 FEET |
| permeability-1 = | 72.000 MD | <u>Static-Data and Constants</u> | |
| permeability-2 = | 300.00 MD | Volume-Factor = | 2.770 vol/vol |
| omega = | 0.032967 | Thickness = | 91.00 FEET |
| Layer (P2-P1) = | -178.00 PSI | Viscosity = | 0.1680 CP |
| Perm-Thickness = | 26616. MD-FEET | Total Compress = | .1917E-04 1/PSI |
| +x boundary(1) = | 1750. FEET (1.00) | Rate = | 5000. STB/D |
| -x boundary(1) = | 1750. FEET (1.00) | Storivity = | 0.0003664 FEET/PSI |
| +y boundary(1) = | 4000. FEET (1.00) | Diffusivity = | 114000. FEET^2/HR |
| -y boundary(1) = | 4000. FEET (1.00) | Gauge Depth = | N/A FEET |
| +x boundary(2) = | 1750. FEET (1.00) | Perf. Depth = | N/A FEET |
| -x boundary(2) = | 1750. FEET (1.00) | Datum Depth = | N/A FEET |
| +y boundary(2) = | 4000. FEET (1.00) | <u>Analysis-Data ID: DATA</u> | |
| -y boundary(2) = | 4000. FEET (1.00) | PFA Starts: 2010-04-26 01:01:01 | |
| Initial Press. = | 12028.0 PSI | PFA Ends : 2010-05-25 05:01:01 | |
| Average Press. = | 11666.4 PSI | | |
| Pore-Volume = | .5351E+09 FEET^3 | | |

Single-layer Oil Reservoir Pressure Build-up Cases (25,000 bopd)



Homogeneous Reservoir

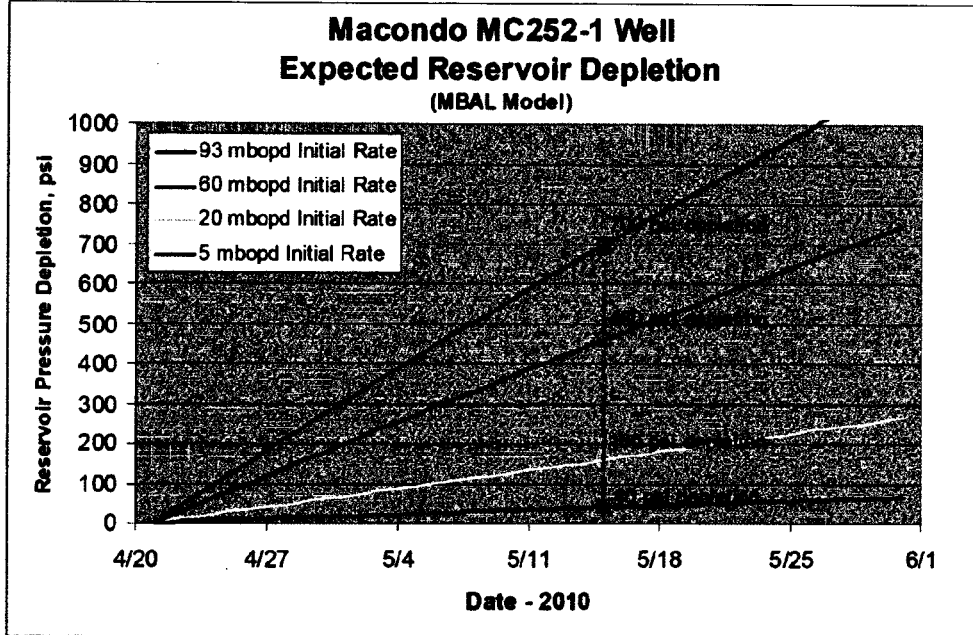
** Simulation Data **

well. storage = 0.10000
 skin = 0. 50.000 ()
 permeability = 300.00 170.00
 Areal Ky/Kx = 1.0000
 Perm-Thickness = 26400. 14960.
 -x boundary = 1750.
 -x boundary = 1.00
 -x boundary = 1750.
 -x boundary = 1.00
 -y boundary = 4000.
 -y boundary = 1.00
 -y boundary = 4000.
 -y boundary = 1.00
 Initial Press. = 11850.0
 Average Press. = 10370.2
 Pore-Volume = .5174E+09

Static-Data and Constants

BBLs/PSI Volume-Factor = 2.770 vol/vol
 MD Thickness = 88.00 FEET
 MD Viscosity = 0.1680 CP
 MD Total Compress = .1917E-04 1/PSI
 MD-FEET Rate = 25000. STB/D
 FEET Storivity = 0.3003543 FEET/PSI
 FOG-FACTOR Diffusivity = 117000. FEET^2/HR
 FEET Gauge Depth = N/A FEET
 FOG-FACTOR Perf. Depth = N/A FEET
 FEET Datum Depth = N/A FEET
 FOG-FACTOR Analysis-Data ID: DATA
 FEET PFA Starts: 2010-04-26 31:01:01
 FOG-FACTOR PFA Ends : 2010-05-25 05:01:01
 PSI
 PSI
 FEET^3

Summary of Pressure Depletion Calculations



Selected PVT data from Al-Marhoun correlations in PROSPER by Tony Liao:

PVT CALCULATIONS #

| Temperature (deg F) | Pressure (psig) | Bubble Point (psig) | Gas Oil Ratio (scf/STB) | Oil Density (g/cc) | Oil Viscosity (centipoise) | Oil FVF (RB/STB) | Oil Compress (1/psi) | Gas Density (g/cc) | Gas Viscosity (centipoise) | Gas FVF (RB/scf) | Z Factor |
|---------------------|-----------------|---------------------|-------------------------|--------------------|----------------------------|------------------|----------------------|--------------------|----------------------------|------------------|----------|
| 40 | 500 | 3634 | 155 | 0.8573 | 93.7590 | 1.0222 | 2.0324E-04 | 0.6413 | 0.0107 | 0.02313 | 0.842 |
| 40 | 1057 | 3634 | 462 | 0.8009 | 20.8526 | 1.1632 | 2.1662E-04 | 0.1174 | 0.0142 | 0.00813 | 0.840 |
| 40 | 1695 | 3634 | 844 | 0.7516 | 8.4904 | 1.3219 | 2.2241E-04 | 0.2128 | 0.0219 | 0.00449 | 0.542 |
| 40 | 2292 | 3634 | 1285 | 0.7074 | 4.8022 | 1.5103 | 2.2312E-04 | 0.2713 | 0.0291 | 0.00352 | 0.574 |
| 40 | 2889 | 3634 | 1775 | 0.6677 | 2.9193 | 1.7247 | 2.2068E-04 | 0.3040 | 0.0345 | 0.00314 | 0.645 |
| 40 | 3487 | 3634 | 2306 | 0.6319 | 2.0401 | 1.9554 | 2.1612E-04 | 0.3256 | 0.0387 | 0.00293 | 0.726 |
| 40 | 4084 | 3634 | 2820 | 0.6082 | 1.5541 | 2.2211 | 3.2633E-05 | 0.3415 | 0.0421 | 0.00280 | 0.810 |
| 40 | 4682 | 3634 | 2020 | 0.6164 | 1.6493 | 2.1977 | 2.8482E-05 | 0.3641 | 0.0451 | 0.00270 | 0.895 |
| 40 | 5279 | 3634 | 2920 | 0.6227 | 1.7545 | 2.1622 | 2.5268E-05 | 0.3646 | 0.0478 | 0.00262 | 0.980 |
| 40 | 5876 | 3634 | 2920 | 0.6285 | 1.8680 | 2.1421 | 2.2706E-05 | 0.3737 | 0.0503 | 0.00255 | 1.064 |
| 40 | 6474 | 3634 | 2820 | 0.6334 | 1.9883 | 2.1258 | 2.0615E-05 | 0.3816 | 0.0525 | 0.00250 | 1.148 |
| 40 | 7071 | 3634 | 2820 | 0.6374 | 2.1137 | 2.1124 | 1.8677E-05 | 0.3896 | 0.0547 | 0.00246 | 1.231 |
| 40 | 7668 | 3634 | 2920 | 0.6408 | 2.2429 | 2.1011 | 1.7410E-05 | 0.3950 | 0.0567 | 0.00242 | 1.313 |
| 40 | 8266 | 3634 | 2920 | 0.6438 | 2.3743 | 2.0915 | 1.6164E-05 | 0.4008 | 0.0586 | 0.00238 | 1.395 |
| 40 | 8863 | 3634 | 2920 | 0.6463 | 2.5064 | 2.0832 | 1.5067E-05 | 0.4062 | 0.0604 | 0.00235 | 1.475 |
| 40 | 9461 | 3634 | 2920 | 0.6486 | 2.6377 | 2.0760 | 1.4117E-05 | 0.4112 | 0.0621 | 0.00232 | 1.556 |
| 40 | 10058 | 3634 | 2920 | 0.6505 | 2.7670 | 2.0697 | 1.3290E-05 | 0.4158 | 0.0638 | 0.00230 | 1.635 |
| 40 | 10655 | 3634 | 2920 | 0.6523 | 2.8929 | 2.0641 | 1.2536E-05 | 0.4202 | 0.0654 | 0.00227 | 1.714 |
| 40 | 11253 | 3634 | 2920 | 0.6539 | 3.0143 | 2.0591 | 1.1871E-05 | 0.4243 | 0.0670 | 0.00225 | 1.792 |
| 40 | 11850 | 3634 | 2020 | 0.6563 | 3.1299 | 2.0546 | 1.1274E-05 | 0.4282 | 0.0685 | 0.00223 | 1.870 |

 # PVT CALCULATIONS #
 #####

| Temperature (deg F) | Pressure (psig) | Bubble Point (psig) | Gas Oil Ratio (scf/STB) | Oil Density (g/cc) | Oil Viscosity (centipoise) | Oil FVF (RB/STB) | Oil Compress (1/psi) | Gas Density (g/cc) | Gas Viscosity (centipoise) | Gas FVF (R3/scf) | Z Factor |
|---------------------|-----------------|---------------------|-------------------------|--------------------|----------------------------|------------------|----------------------|--------------------|----------------------------|------------------|----------|
| 160 | 500 | 5290 | 103 | 0.7887 | 1.2674 | 1.0999 | 1.3548E-04 | 0.0302 | 0.0127 | 0.03156 | 0.926 |
| 160 | 1097 | 5290 | 309 | 0.7544 | 0.7364 | 1.1962 | 1.4516E-04 | 0.0712 | 0.0141 | 0.01340 | 0.850 |
| 160 | 1695 | 5290 | 565 | 0.7237 | 0.5044 | 1.3071 | 1.5143E-04 | 0.1167 | 0.0163 | 0.00818 | 0.797 |
| 160 | 2292 | 5290 | 861 | 0.6905 | 0.3788 | 1.4326 | 1.5516E-04 | 0.1609 | 0.0192 | 0.00593 | 0.780 |
| 160 | 2889 | 5290 | 1190 | 0.6690 | 0.3008 | 1.6726 | 1.5679E-04 | 0.1990 | 0.0223 | 0.00480 | 0.795 |
| 160 | 3487 | 5290 | 1546 | 0.6442 | 0.2478 | 1.7273 | 1.5897E-04 | 0.2298 | 0.0254 | 0.00415 | 0.829 |
| 160 | 4084 | 5290 | 1928 | 0.6209 | 0.2094 | 1.8957 | 1.5902E-04 | 0.2546 | 0.0284 | 0.00379 | 0.877 |
| 160 | 4682 | 5290 | 2332 | 0.5990 | 0.1802 | 2.0810 | 1.5417E-04 | 0.2747 | 0.0311 | 0.00348 | 0.931 |
| 160 | 5279 | 5290 | 2758 | 0.5784 | 0.1574 | 2.2831 | 1.5168E-04 | 0.2913 | 0.0336 | 0.00328 | 0.989 |
| 160 | 5876 | 5290 | 3220 | 0.5799 | 0.1601 | 2.3216 | 2.4209E-05 | 0.3054 | 0.0359 | 0.00313 | 1.050 |
| 160 | 6474 | 5290 | 3474 | 0.5674 | 0.1709 | 2.2920 | 2.3796E-05 | 0.3175 | 0.0381 | 0.00301 | 1.112 |
| 160 | 7071 | 5290 | 3920 | 0.5937 | 0.1824 | 2.2678 | 2.1790E-05 | 0.3261 | 0.0401 | 0.00291 | 1.176 |
| 160 | 7668 | 5290 | 3920 | 0.5991 | 0.1943 | 2.2475 | 2.0096E-05 | 0.3375 | 0.0420 | 0.00283 | 1.239 |
| 160 | 8266 | 5290 | 3920 | 0.6037 | 0.2065 | 2.2303 | 1.8646E-05 | 0.3469 | 0.0437 | 0.00276 | 1.303 |
| 160 | 8863 | 5290 | 3920 | 0.6077 | 0.2190 | 2.2155 | 1.7392E-05 | 0.3535 | 0.0454 | 0.00270 | 1.367 |
| 160 | 9461 | 5290 | 3920 | 0.6113 | 0.2314 | 2.2026 | 1.6296E-05 | 0.3605 | 0.0471 | 0.00265 | 1.431 |
| 160 | 10058 | 5290 | 3920 | 0.6144 | 0.2438 | 2.1914 | 1.5329E-05 | 0.3670 | 0.0486 | 0.00260 | 1.494 |
| 160 | 10655 | 5290 | 3920 | 0.6172 | 0.2560 | 2.1814 | 1.4470E-05 | 0.3729 | 0.0501 | 0.00256 | 1.557 |
| 160 | 11253 | 5290 | 3920 | 0.6197 | 0.2679 | 2.1726 | 1.3703E-05 | 0.3785 | 0.0516 | 0.00252 | 1.620 |
| 160 | 11850 | 5290 | 3920 | 0.6220 | 0.2794 | 2.1646 | 1.3013E-05 | 0.3837 | 0.0530 | 0.00249 | 1.683 |

 # PVT CALCULATIONS #
 #####

| Temperature (deg F) | Pressure (psig) | Bubble Point (psig) | Gas Oil Ratio (scf/STB) | Oil Density (g/cc) | Oil Viscosity (centipoise) | Oil FVF (RB/STB) | Oil Compress (1/psi) | Gas Density (g/cc) | Gas Viscosity (centipoise) | Gas FVF (R3/scf) | Z Factor |
|---------------------|-----------------|---------------------|-------------------------|--------------------|----------------------------|------------------|----------------------|--------------------|----------------------------|------------------|----------|
| 240 | 500 | 6455 | 192 | 0.7462 | 0.8087 | 1.1576 | 1.0729E-04 | 0.0261 | 0.0141 | 0.03663 | 0.952 |
| 240 | 1097 | 6455 | 268 | 0.7208 | 0.4611 | 1.2371 | 1.1493E-04 | 0.0592 | 0.0151 | 0.01614 | 0.906 |
| 240 | 1695 | 6455 | 461 | 0.6961 | 0.3421 | 1.3272 | 1.2033E-04 | 0.0940 | 0.0166 | 0.01019 | 0.877 |
| 240 | 2292 | 6455 | 687 | 0.6771 | 0.2705 | 1.4279 | 1.2419E-04 | 0.1263 | 0.0185 | 0.00744 | 0.867 |
| 240 | 2889 | 6455 | 949 | 0.6571 | 0.2227 | 1.5399 | 1.2668E-04 | 0.1600 | 0.0206 | 0.00599 | 0.875 |
| 240 | 3487 | 6455 | 1234 | 0.6381 | 0.1884 | 1.6508 | 1.2799E-04 | 0.1878 | 0.0229 | 0.00506 | 0.899 |
| 240 | 4084 | 6455 | 1534 | 0.6199 | 0.1626 | 1.7525 | 1.2851E-04 | 0.2119 | 0.0251 | 0.00450 | 0.933 |
| 240 | 4682 | 6455 | 1851 | 0.6025 | 0.1423 | 1.8369 | 1.2855E-04 | 0.2326 | 0.0273 | 0.00410 | 0.973 |
| 240 | 5279 | 6455 | 2201 | 0.5868 | 0.1260 | 1.9097 | 1.2746E-04 | 0.2505 | 0.0294 | 0.00381 | 1.019 |
| 240 | 5876 | 6455 | 2596 | 0.5698 | 0.1126 | 1.9760 | 1.2646E-04 | 0.2660 | 0.0314 | 0.00359 | 1.068 |
| 240 | 6474 | 6455 | 2920 | 0.5561 | 0.1016 | 2.0294 | 1.2591E-04 | 0.2797 | 0.0333 | 0.00341 | 1.118 |
| 240 | 7071 | 6455 | 3220 | 0.5630 | 0.1087 | 2.0914 | 1.2573E-04 | 0.2917 | 0.0351 | 0.00327 | 1.171 |
| 240 | 7668 | 6455 | 3220 | 0.6698 | 0.1162 | 2.0630 | 1.1887E-04 | 0.3026 | 0.0368 | 0.00316 | 1.224 |
| 240 | 8266 | 6455 | 3220 | 0.5756 | 0.1238 | 2.0390 | 1.0309E-04 | 0.3123 | 0.0385 | 0.00306 | 1.278 |
| 240 | 8863 | 6455 | 3420 | 0.5807 | 0.1317 | 2.0194 | 1.8941E-05 | 0.3211 | 0.0401 | 0.00297 | 1.333 |
| 240 | 9461 | 6455 | 3920 | 0.5863 | 0.1396 | 2.0005 | 1.7747E-05 | 0.3292 | 0.0416 | 0.00290 | 1.388 |
| 240 | 10058 | 6455 | 3920 | 0.5893 | 0.1475 | 2.2849 | 1.6695E-05 | 0.3366 | 0.0431 | 0.00284 | 1.443 |
| 240 | 10655 | 6455 | 3920 | 0.5928 | 0.1554 | 2.2711 | 1.5760E-05 | 0.3405 | 0.0445 | 0.00278 | 1.498 |
| 240 | 11253 | 6455 | 3920 | 0.5960 | 0.1631 | 2.2599 | 1.4925E-05 | 0.3489 | 0.0459 | 0.00273 | 1.553 |
| 240 | 11850 | 6455 | 3920 | 0.5989 | 0.1706 | 2.2479 | 1.4173E-05 | 0.3559 | 0.0472 | 0.00268 | 1.607 |

